We are IntechOpen, the world's leading publisher of Open Access books
Built by scientists, for scientists

6,900
Open access books available

185,000
International authors and editors

200M
Downloads

154
Countries delivered to

Our authors are among the

TOP 1%
most cited scientists

12.2%
Contributors from top 500 universities

CLARIVATE ANALYTICS
BOOK CITATION INDEX
INDEXED

WEB OF SCIENCE™

Selection of our books indexed in the Book Citation Index
in Web of Science™ Core Collection (BKCI)

Interested in publishing with us?
Contact book.department@intechopen.com

Numbers displayed above are based on latest data collected.
For more information visit www.intechopen.com

Spectral-Structure Activity Relationship (Spectral-SAR) Assessment of Ionic Liquids' in Silico Ecotoxicity

Ana-Maria Putz and Mihai V. Putz

Additional information is available at the end of the chapter

http://dx.doi.org/10.5772/51657

1. Introduction

The use of green solvents, including ionic liquids (IL), in the synthesis of new materials is currently highlighted worldwide [1-5]. The green high thermal stabilities, and can remain in the liquid state over a wide range of temperatures (from -50°C to 200°C). Furthermore, ILs exhibit low toxicity because of their exceptionally low volatility. This property is why ILs could be used as "green" alternatives to volatile organic solvents in many processes [6,7].

Accordingly, ILs have been used as a reaction medium for inorganic materials, which demonstrates the pre-organized structure of the ILs as a template for generating porous nanomaterials [8,9]. It is well-known that the properties and structures of mesoporous materials vary by the choice of synthesis conditions, such as temperature, reagents, base concentrations, and the nature of the organic groups [10]. By organic groups, one means the organic chains and structures that affect the functionality of the precursor; for example, where there is Si-C bond, depending on the silica to surfactant ratio, different pore topologies (hexagonal, cubic and lamellar) are present, and when only ionic liquid was used as the surfactant, mesoporous silica with an irregular shape may be obtained [11]. However, when a small amount of cetyl trimethylammonium bromide (CTAB) was added to the reaction, mesoporous silica with a spherical shape was obtained. When a mixture of ionic liquids and CTAB was used as the surfactant templates, larger mesopores were formed in the silica spheres [12]; however, ILs can generally dramatically decrease the polarity and dielectric constant of water and increase the solubility of surfactants when used as co-solvents [13,14]. However, the interaction between CTAB and IL has also been observed, which causes the IL to behave as a co-surfactant [14]. Starting from these new concepts, ILs with different cations (e.g., imidazolium, pyridinium and ammonium) and anions (e.g., hexafluorophosphate, tetrafluoro-

borate, octyl sulfate and bromide) and the ordinary CTAB and the mixture of CTAB and ILs are used in the synthesis of mesoporous silica.

Furthermore, ILs provide an interesting method for controlling the chemical contents of the collapsing bubble through the reduction of the solvent vapor pressure [15] because the rates of sonochemical reactions can be increased by decreasing the vapor pressure of the solvent or by choosing a less volatile one [16]. ILs are usually more viscous and denser than other organic solvents, and producing cavitations should be more difficult under such conditions with large cohesive forces [16,17].

Studies of the thermal decomposition of ILs confined in nanopores compared to bulky pores are also currently on the forefront of nanomaterials research. Many physicochemical properties of ILs have been observed to change when confined in nanopores, which results from the interaction of the IL cations/anions with the pore walls, which could be weak, as in silica nanopores [18,19]. These studies influence the next step, i.e., the surface functionalization of mesoporous silica materials through the covalent bonding of organic groups, which is achieved through the comparative co-condensation and post-grafting of amino and alkyl functionalized silica alkoxide precursors [20]. Importantly, the comparative study is necessary to optimize the synthesis methods for nanomaterials because, even if the post-grafting method produces well-ordered functionalized mesostructured materials, it often produces non-uniformly distributed organic groups [20]. Furthermore, the co-condensation synthetic method for mesoporous materials involves a one-step procedure and allows better control of the loading and distribution of the organic groups [20], as was detailed in the recent review on the advances in (bio)responsive nanomaterials [21]. Supplementary information on the effects of ILs on the texture of gels can be obtained from the pore size distribution. This aspect is interesting because the ionic liquid concentration changes the pore volume due to the low volatility of the IL, which reduces the surface tension associated with the pore collapse [22-25].

The next step in the ecotoxicological evaluation of the synthetized mesoporous silica is to use the logistic enzyme kinetic and Spectral-SAR methods [26-30] with acetylcholine esterase as a working enzyme. Acetylcholine is a notably good marker for monitoring the evolution in ionic liquids, due to the similar chemical structures of many ionic liquids cations and acetylcholine and especially because this enzyme does not follow the standard Michaelis-Menten kinetics mechanism. The logistic enzyme kinetics [31-35] is an analytical substitute for the Michaelis-Menten mechanism, and it is based on some probabilistic considerations that better accommodate the QSSA (quasi-steady state approximation) conditions, while providing the analytical transformation of the W-Lambert function into a logarithmic function; this so-called logistic transformation was successfully evaluated for different cases of enzyme kinetics [31-39]. The analytical information contained in the logistic enzymatic temporal curves could be further combined with a QSAR algorithm, such as the Spectral-SAR, for designing molecular mechanisms of the ecotoxicity; this procedure has already been applied for bare ILs [27,28,38,40]. Eventually, this procedure is intended to be used for some toxicity tests [41,42] or even for obtaining the efficiency of the material as a drug carrier in biological media, if the proper conditions are satisfied.

Regarding the action/toxicity mechanism of ionic liquids (M.O.A.), possible mechanisms of toxic actions are identified through membrane disruption because they have structural similarity with detergents, pesticides and antibiotics [43-46] that induce polar narcosis, due to their interfacial properties, and may cause membrane-bond protein disruption [47-49]. As a possible mode of action, disrupted membranes and hydrophobic molecules have a greater ability to accumulate at this interface [50]. The low K_{ow} values of imidazolium ionic liquids indicate the low permeability of these ionic liquids [47]. However, other mechanisms arise from acethylcolinesterase inhibition [51], relate to a common cellular structure or process [45], involve structural DNA damage [47,52], or are mediated by certain bacteria that could potentially break down imidazolium into different metabolites that could be inhibited by the ionic liquid itself [43,44]. Nevertheless, knowing if the chemicals could reach the target site in the organism and by which mechanism is of paramount importance, and at minimum, a conceptual extrapolation from *in vitro* to *in vivo* studies is required [51] because other factors, such as biodegradation and bioaccumulation, are necessary before conclusions can be drawn [49].
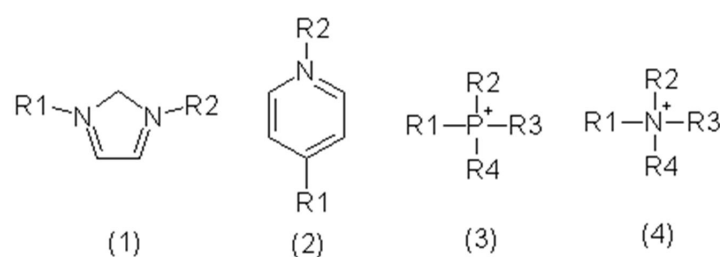

Figure 1. The four most important classes of ionic liquids based on the reference cation: (1) imidazolium, (2) pyridinium-, (3) phosphonium-, (4) ammonium- [39].

The dose-response approach for estimating the lethal effects of toxicants on organisms is being criticized because of the lack of real ecological meaning; furthermore, regulatory norms have been established around LC50 values that can be compared between different toxicants and organisms [47,53]. In this respect, it was observed that the side chain toxic mode of action of ionic liquids is not specific to species, and a similar relationship has been observed [47]. However, the systematic variation of, for instance, R1 and R2 at identical head groups and anions from the molecular to individual organism level lead to the conclusion in most published data that the shorter the chain lengths of the side chains, the lower the cytotoxicity (higher EC50 values) [50,54]. The electronic portion of the bond factor extends along a chain that has no more than 5 alkane carbons, which results in a decrease in the overall hydrophobicity; therefore, chains longer than 5-6 carbon atoms will have a considerably greater permeability through the cell membrane (for example, [DMIM][BF4]), see ref. [55]. Therefore, chemical transformations of the side chains of ionic liquids may reduce their toxicity because the metabolites are less toxic compared to their parent chemicals [54]. With respect to the cationic effects, see Figure 1, the imidazolium ring plays a major role due its structure as a delocalized aromatic system with a high electron acceptor potential; therefore, the nitrogen atoms are not capable of forming any hydrogen bonds, which results in a rigid

and sterically hindered system. The elongation of the R2 residue causes a continuous increase of flexibility, which implies more conformational freedom [56]. The chemical nature of a head group also influences the biological activity [54]. The fragmental hydrophobicity of each carbon connected to a quaternary amine combines a geometric bond factor that applies to the neutral solute together with a negative electronic bond factor, which decreases in magnitude with the square of the distance from the central nitrogen atom [55,57]. Complementarily, the anion could play a central role as a technicophore because it exhibits a high potential for changing the materials technological properties (solubility, viscosity); however, there are reports that the anion presents no significant effects [44,45,55]. The first study reporting the influence of the anion was by the Jastorff group [54], where it was reported that the anion in the ion pair can partially decompose, as was previously observed [55,58,59].

Finally, at the computational level, the detailed examination of the relative energies and structural interactions (such as ion position, H-bonding and variability in the anion conformation) in gas-phase ion-pairs has emphasized how these quantities can be used to construct a picture of the local structure and interactions that occur in ionic liquids. For instance, [BMIM][Cl] (1-n-butyl-3-methylimidazolium chloride) forms a highly connected liquid with relatively strong interactions, [BMIM][TFMSi] (1-n-butyl-3-methylimidazolium bis(trifluoromethylsulfonyl)imide) forms a low connectivity network of weakly linked ions, whereas [BMIM][BF4] lies between these extremes and forms a weak but more regular network. The melting points and viscosity are somewhat dependent on the local interactions between an ion and other molecules in the first solvation shell. For imidazolium based cations, nine sites of interactions are preferred by the anion [60-63]. Hunt et al. demonstrated that the hydrogen bond is primarily ionic with a moderate covalent character. The fact that the Coulombic attraction is the dominant stabilization force was demonstrated by analyzing the charge distribution, molecular orbitals and electron density of the dimer complex [BMIM][Cl] [63]. The interactions governing the top conformers are notably different compared to those where the Cl anion remains in-plane (where the Cl anion interacts with the π-manifold of the orbitals); the LUMO of the ion-pair is the cation antibonding orbital; therefore, electron acceptance is not favorable [63]. The effect of the chloride anion on the rotation of the butyl chain was consequently investigated and observed to lower certain rotational barriers while enhancing others [61]. The Coulombic forces in an ionic liquid, and hence the point charges or charge distribution on the constituent ions are anticipated to be more important than in liquids composed of neutrally charged molecules [60]; these ions allow a type of semi-classical analysis for the toxicity of ILs, which is well-adapted for quantitative structure-activity studies (QSAR), to which the present review belongs. Nevertheless, even the well-regarded QSAR methodology has to be refined and adapted or extended to include the chemical electrostatic interactions present in the IL and of their transduction into various organism triggering (or not) toxicity. These aspects will be reviewed and exemplified in the following.

2. QSAR/Spectral-SAR Modeling of the Structure-EcoToxicity of Ionic Liquids

It is an already established fact that the costs of all approaches for sustainable product design can be reduced using the SAR and QSAR methods [56]. For instance, the anti-microbial activity of quaternary ammonium chlorides is dependent on the lipophilicity, and the 1-octanol-water partition coefficient, K_{ow}, could provide a good approximation for the lipophilicity of the compound. The relationship between the chemical structure and anti-microbial activity of several new choline-like quaternary ammonium derivatives was analyzed using the QSAR method, and all of the studied compounds were active against the microorganisms. The statistically significant correlation of the obtained QSAR equations confirms that the lipophilicity is the primary factor that governs anti-microbial activity [43]. The octanol-water partition coefficient has been correlated with bioaccumulation and toxicity in fish and to sorption in soil and sediments. The K_{ow} values for the BMIM cation range from 0.003 to 1.1, depending on the choice of anion, and the K_{ow} value increases with increasing length of the alkyl chain on the cation. Replacing the H atom between the 2 nitrogen atoms in the ring with a methyl group has almost no effect on the K_{ow} value. Because all of the measured K_{ow} values in the analyzed ionic liquids, i.e., imidazolium ionic liquids with butyl, ethyl, dimethyl, hexyl and octyl side chains with different anions, such as tetrafluoroborate, nitrate, bis(trifluoromethylsulfonyl)imide), are less than 15, these ionic liquids will not accumulate or concentrate in the environment. It was also observed that the K_{ow} values for ionic liquids with the TFMSi (bis(trifluoromethylsulfonyl)imide) anion (a notably hydrophobic anion) are dependent on concentration, even at the diluted concentrations studied [64].

However, QSPRs (Quantitative Structure Properties Relationships) methods could be used to correlate and predict the toxicity of ionic liquids. With at most 4 molecular descriptors, log EC50 and log EC5 data are reproduced with a R^2 (statistical Pearson correlation coefficient) of 0.78-0.88 using tests with *Vibrio fischeri* and *Daphnia magna*. These methods calculated the electronic, spatial, structural, thermodynamic and topological descriptors for both the cation and anion *separately*, whereas the geometries were also optimized *separately*. Concerning *Vibrio fischeri*, the QSPR equations that used cationic (first equation) and cationic + anionic (second equations) descriptors fit the training set well, with $R^2=0.887$ and $R^2=0.782$, respectively. However, the majority of the training set compounds were imidazolium and pyridinium based ionic liquids. Then, Couling and co-workers [49] used the equation to predict the toxicity of new compounds, which contained ammonium and phosphonium cations, but the toxicity of these new additional compounds was not predicted with the same accuracy, which led to the conclusion that the equation is only good for compounds of the same class. The best accuracy for a new predicted compound (using the first QSPR equation) was for [BdMAPy][Br] (1-n-butyl-4-dimethylaminopyridinium bromide) because it contains an aromatic pyridinium cation, and it also contains an amino group, unlike all of the other training set compounds. Concerning *Daphnia magna*, the QSPR equation fits the training data set well ($R^2=0.862$), and the descriptors are similar to those provided for *Vibrio fischeri*, which suggests that there may be similar indicators of toxicity observed in many different

species. The equation was used to predict the toxicity of another compound, and contrary to the case of *Vibrio fischeri*, the correlation was good, $R^2=0.775$; however, the neglected compounds were more similar to those of the training set compounds [49]. Such results further motivated the use of the actual Spectral-SAR method for these two paradigmatic species response upon IL action because it is an important step in constructing a consistent ecotoxicological test battery. The reliability of the Spectral-SAR/QSAR studies primarily relies on the lack of readily accessible ecotoxicological data [65]. Note that because the principles of green chemistry state that one should consider the entire process (life cycle analysis), rather than the individual components of a reaction (single issue sustainability), the acute toxicity measurements do not fully characterize the full impact of the release of a substance into the environment, but they are only part of the environmental impact assessment [65,66]. In particular, ionic liquids with cations, such as pyridinium, imidazolium and pyrrolidinium, have been nominalized by the United States National Toxicology Program (NTP) for toxicological testing because of their potential use as new solvents and potential to enter the aquatic system [67]: if an accidental discharge of ionic liquids into water were to occur, there may be an environmental risk to aquatic plants and animals because many of the ILs are water-soluble [48]. The recorded averaged descriptions of the acute toxicity based on the LC50 (mg/mL) are very highly toxic ($<10^{-4}$), highly toxic (10^{-4}-10^{-3}), moderately toxic (10^{-3}-10^{-2}), slightly toxic (10^{-2}-10^{-1}) and not acutely toxic ($>10^{-1}$) [55,68].

3. Algebraic QSAR: Spectral-SAR [69,70]

The key concept in the SAR discussion concerns the algebraic consideration of biological activity and the structural parameters in Table 1. As a consequence, we may further employ this feature to quantify the basic SAR through an *orthogonal* space. The idea is to transform the columns of structural data in Table 1 into an abstract orthogonal space, where all of the predictor variables are independent, solve the SAR problem in orthogonal space and subsequently compare the result to the initial data using a coordinate transformation. Because QSAR models aim to develop correlations between the molecular structures of interest and the measured (or otherwise evaluated) activity, it naturally appears that the *structure* part of the problem is accommodated within quantum theory and its formalisms.

Activity		Structural predictor variables				
$\lvert Y_{OBS(ERVED)} \rangle$	$\lvert X_0 \rangle$	$\lvert X_1 \rangle$	...	$\lvert X_k \rangle$	...	$\lvert X_M \rangle$
$y_{1\text{-}OBS}$	1	x_{11}	...	x_{1k}	...	x_{1M}
$y_{2\text{-}OBS}$	1	x_{21}	...	x_{2k}	...	x_{2M}
$\vdots$	$\vdots$	$\vdots$	$\vdots$	$\vdots$	$\vdots$	$\vdots$
$y_{N\text{-}OBS}$	1	x_{N1}	...	x_{Nk}	...	x_{NM}

Table 1. The vectorial descriptors in a Spectral-SAR analysis.

In fact, there are a few quantum characteristics that we are using within the present approach [29]:

• Any molecular structural state (dynamical because it undergoes interactions with the species and organisms) may be represented by a $|ket\rangle$ *state vector* in an abstract Hilbert space, which follows the $\langle bra|ket\rangle$ Dirac formalism [71]; such states are to be represented using any reliable molecular index, or specifically, in our study, by the hydrophobicity $|LogP\rangle$, polarizability $|POL\rangle$, and the total optimized energy $|E_{tot}\rangle$. These parameters are only the so-called Hansch parameters, which are usually employed to account for the diffusion, electrostatic and steric effects for molecules acting, for instance, within the cells of organisms, respectively;

• The (quantum) *superposition principle*, which ensures that the summation of molecular states map onto another resulting molecular state, which is interpreted here as the bio-, eco- or toxico- logical activity, e.g., $|Y\rangle = |X_0\rangle + c_1|X_1\rangle + ... + c_M|X_M\rangle$, where $|X_0\rangle$ represents the "noise" activity (present even when all other influences are absent);

• The *orthogonalization feature* of quantum states, which is a crucial condition where the superimposed molecular states generate other molecular states (here quantified as the activity of the molecular ligand - linking receptor); analytically, the orthogonalization condition is represented by the $\langle bra|ket\rangle$ scalar product of two envisaged states (molecular indices). If $\langle bra|ket\rangle = 0$, then the states are said to be orthogonal, and the molecular descriptors are independent; therefore, they are suitable to be added as contributing states in the resulting activity and as molecular indices in the activity correlation.

As such, the analytical procedure is decomposed into three fundamental steps.

I.   Given a set of N molecules that are being examined for their biological activity, they produce through the considered M structural indicators all of the input information (the states) that may be vectorially expressed by the columns in Table 1 and correlated through the following equation:

$$\left|Y_{OBS(ERVED)}\right\rangle = b_0\left|X_0\right\rangle + b_1\left|X_1\right\rangle + ... + b_k\left|X_k\right\rangle + ... + b_M\left|X_M\right\rangle + \left|prediction\ error\right\rangle$$
$$= \left|Y_{PRED(ICTED)}\right\rangle + \left|prediction\ error\right\rangle \tag{1}$$

with

$$\left|X_0\right\rangle = \left|1\ 1\ \cdots\ 1_N\right\rangle \tag{2}$$

added to account for the noise term. For equation (1) to represent a reliable model of the given activities, the assumed molecular states (indices) should constitute an orthogonal set; having this constraint is a quantum mechanical fundamental, as described above. However, unlike other important studies that have addressed this problem [72,73], the present use of

the Spectral-SAR method assumes that the prediction error vector in eq. (1) arises from the predicted activity's being orthogonal because it cannot consider the input data otherwise

$$\langle Y_{PRED} | prediction\ error \rangle = 0 \tag{3}$$

being not known *a priori* any correlation is made. In this manner, it follows from eqs. (1) and (3) that the prediction error vector has to be orthogonal on all other descriptor states of the predicted activity.

$$\langle X_{i=\overline{0,M}} | prediction\ error \rangle = 0 \tag{4}$$

In other words, conditions (3) and (4) confirm the form of (1) in the sense that the prediction vector and the prediction activity $| Y_{PRED} \rangle$ (with all of its sub-intended states $| X_{i=\overline{0,M}} \rangle$) belong to disjointed (thus orthogonal) Hilbert spaces; that is, one can state that the Hilbert space of the observed activity $| Y_{OBS} \rangle$ may be decomposed into a predicted and an error independent Hilbert sub-spaces of states. Therefore, within the *Spectral-SAR* procedure, the first step in the orthogonalization procedure orthogonalizes the predicted activity to its prediction error, whereas the remaining orthogonalization algorithm does not search for optimizing the minimization of errors, but it searches for the optimum method for producing the ideal correlation between $| Y_{PRED} \rangle$ and the given descriptors $| X_{i=\overline{0,M}} \rangle$.

II.   Next, the Gram-Schmidt orthogonalization algorithm is applied by constructing the orthogonal set of descriptors using the consecrated iteration [74-76]

$$|\Omega_0\rangle = |X_0\rangle \tag{5}$$

$$|\Omega_k\rangle = |X_k\rangle - \sum_{i=0}^{k-1} r_i^k |\Omega_i\rangle \tag{6}$$

$$r_i^k = \frac{\langle X_k | \Omega_i \rangle}{\langle \Omega_i | \Omega_i \rangle}, k = \overline{1,M} \tag{7}$$

providing the orthogonal correlation

$$|Y_{PRED}\rangle = \omega_0 |\Omega_0\rangle + \omega_1 |\Omega_1\rangle + ... + \omega_k |\Omega_k\rangle + ... + \omega_M |\Omega_M\rangle \tag{8}$$

$$\omega_k = \frac{\langle \Omega_k | Y \rangle}{\langle \Omega_k | \Omega_k \rangle}, k = \overline{0,M} \tag{9}$$

III.   Remarkably, while the studies dedicated to the orthogonal problem usually stop at this stage, the Spectral-SAR method uses this stage to provide the solution for the original searched correlation, eq. (1). This process can be adequately achieved by rearranging eqs. (6) and (8) such that the system of all descriptors in Table 1 can be written in terms of orthogonal descriptors

$$
\begin{cases}
|Y_{PRED}\rangle = \omega_0 |\Omega_0\rangle + \omega_1 |\Omega_1\rangle + ... + \omega_k |\Omega_k\rangle + ... + \omega_M |\Omega_M\rangle \\
|X_0\rangle = 1 \cdot |\Omega_0\rangle + 0 \cdot |\Omega_1\rangle + ... + 0 \cdot |\Omega_k\rangle + ... + 0 \cdot |\Omega_M\rangle \\
|X_1\rangle = r_0^1 |\Omega_0\rangle + 1 \cdot |\Omega_1\rangle + ... + 0 \cdot |\Omega_k\rangle + ... + 0 \cdot |\Omega_M\rangle \\
\text{..} \\
|X_k\rangle = r_0^k |\Omega_0\rangle + r_1^k |\Omega_1\rangle + ... + 1 \cdot |\Omega_k\rangle + ... + 0 \cdot |\Omega_M\rangle \\
\text{..} \\
|X_M\rangle = r_0^M |\Omega_0\rangle + r_1^M |\Omega_1\rangle + ... + r_k^M |\Omega_k\rangle + ... + 1 \cdot |\Omega_M\rangle
\end{cases}
\tag{10}
$$

System (10) has no trivial (orthogonal) solution if and only if the associated extended determinant vanishes; this condition introduces the Spectral-SAR determinant and its equation [26]

$$
\begin{Vmatrix}
|Y_{PRED}\rangle & \omega_0 & \omega_1 & \cdots & \omega_k & \cdots & \omega_M \\
|X_0\rangle & 1 & 0 & \cdots & 0 & \cdots & 0 \\
|X_1\rangle & r_0^1 & 1 & \cdots & 0 & \cdots & 0 \\
\vdots & \vdots & \vdots & \vdots & & \vdots & \\
|X_k\rangle & r_0^k & r_1^k & \cdots & 1 & \cdots & 0 \\
\vdots & \vdots & \vdots & \vdots & & \vdots & \\
|X_M\rangle & r_0^M & r_1^M & \cdots & r_k^M & \cdots & 1
\end{Vmatrix} = 0
\tag{11}
$$

If the determinant of eq. (11) is expanded on its first column, and the result rearranged so that to have $|Y_{PRED}\rangle$ on the left side and the rest of states/indicators on the right side, the searched QSAR solution of the initial problem of eq. (1) is obtained as the Spectral-SAR vectorial expansion (from where the "spectral" name is also justified) with the error vector already absorbed in the orthogonalization procedure. In fact, the Spectral-SAR procedure uses double conversion passages: one forward from the given problem of eq. (1) to the orthogonal one of eq. (8) where the error vector is orthogonally "dissolved"; and the reverse one, back from the orthogonal to the real descriptors throughout the system (10), which provides the determinant (11) to be expanded as the QSAR solution.

The result is that the QSAR/Spectral-SAR equation is now directly delivered by the determinant (11) and not through matrices products, as in the statistical Pearson approach, while directly providing the Spectral-SAR correlation equation and not only the parameters of multi-variate correlation [77-83]. Furthermore, the Spectral-SAR algorithm is also *invariant*

to the order of descriptors that are chosen in orthogonalization procedure, which provides equivalent determinants only with rearranged lines; this is a matter that was not previously achieved by other orthogonalization techniques [84-87].

However, it is worth being convinced by comparing the present Spectral-SAR method with the standard statistical one by specializing the general problem (1) to the linear case

$$|Y_{PRED}\rangle = b_0|X_0\rangle + b_1|X_1\rangle \tag{12}$$

and to determine whether it furnishes the linear regression parameters given by the consecrated least squares analysis through the Spectra-SAR equation (11) [81-83]. In this respect, we actually deal with the particular equation

$$0 = \begin{vmatrix} \|Y_{PRED}\rangle & \omega_0 & \omega_1 \\ |X_0\rangle & 1 & 0 \\ |X_1\rangle & r_0^1 & 1 \end{vmatrix} = |Y_{PRED}\rangle \begin{vmatrix} 1 & 0 \\ r_0^1 & 1 \end{vmatrix} - |X_0\rangle \begin{vmatrix} \omega_0 & \omega_1 \\ r_0^1 & 1 \end{vmatrix} + |X_1\rangle \begin{vmatrix} \omega_0 & \omega_1 \\ 1 & 0 \end{vmatrix} \tag{13}$$

which is immediately rearranged to

$$|Y_{PRED}\rangle = \underbrace{\left(\omega_0 - r_0^1\omega_1\right)}_{b}|X_0\rangle + \underbrace{\omega_1}_{a}|X_1\rangle \tag{14}$$

such that identifying the actual linear coefficients

$$a = \omega_1 \tag{15}$$

$$b = \omega_0 - r_0^1\omega_1 \tag{16}$$

When evaluating expressions (15) and (16) within the Spectral-SAR algorithm, there are instructions to identify only the relevant variables from Table 1 using the convenient notation

$|Y_{PRED}\rangle$	$|X_0\rangle$	$|X_1\rangle$
y_1	1	x_1
y_2	1	x_2
⋮	⋮	⋮
y_N	1	x_N

Other working tools are the zero-th and the first orthogonal vectors, which are accordingly considered and computed as (5) with (2) and respectively by.

$$|\Omega_1\rangle = |X_1\rangle - r_0^1 |\Omega_0\rangle$$
$$= |x_1 \ x_2 \ ... \ x_N\rangle - \frac{1}{N}\sum_{i=1}^{N} x_i |1\ 1\ 1 \ ...\ 1\rangle = \left|x_1 - \frac{1}{N}\sum_{i=1}^{N} x_i \ ... \ x_N - \frac{1}{N}\sum_{i=1}^{N} x_i\right\rangle \tag{17}$$

with the help of the coefficient

$$r_0^1 = \frac{\langle X_1 | \Omega_0\rangle}{\langle \Omega_0 | \Omega_0\rangle} = \frac{1}{N}\sum_{i=1}^{N} x_i \tag{18}$$

specialized from the general definition (7).

In the same manner, the other specific Spectral-SAR coefficients from the general orthogonal recipe (9) are now computed as the zero-th order contribution for linear regression

$$\omega_0 = \frac{\langle \Omega_0 | Y\rangle}{\langle \Omega_0 | \Omega_0\rangle} = \frac{1}{N}\sum_i y_i \tag{19}$$

whereas the first order contribution precisely recovers the linear slope [69,70]

$$\omega_1 = \frac{\langle \Omega_1 | Y\rangle}{\langle \Omega_1 | \Omega_1\rangle}$$
$$= \frac{\langle x_1 - N^{-1}\sum x_i \ ... \ x_N - N^{-1}\sum x_i | y_1 \ ... \ y_N\rangle}{\sum_i \left(x_i - N^{-1}\sum_i x_i\right)^2}$$
$$= \frac{\sum_i y_i \left(x_i - N^{-1}\sum_i x_i\right)}{\sum_i \left(x_i - N^{-1}\sum_i x_i\right)^2} = \frac{\sum_i y_i x_i - N^{-1}\left(\sum_i y_i\right)\left(\sum_i x_i\right)}{\sum_i \left[x_i^2 + N^{-2}\left(\sum_i x_i\right)^2 - 2N^{-1}x_i\sum_i x_i\right]} \tag{20}$$
$$= \frac{N\sum_i y_i x_i - \left(\sum_i y_i\right)\left(\sum_i x_i\right)}{N\sum_i x_i^2 - \left(\sum_i x_i\right)^2} = a$$

as prescribed by the correspondence of (15). Additionally, its companion – the noise term coefficient of eq. (14) - may be now directly evaluated with (16)

$$b = \omega_0 - r_0^1 \omega_1$$

$$= \frac{1}{N}\sum_i y_i - \frac{1}{N}\left(\sum_i x_i\right) \frac{N\sum_i y_i x_i - \left(\sum_i y_i\right)\left(\sum_i x_i\right)}{N\sum_i x_i^2 - \left(\sum_i x_i\right)^2}$$

$$= \frac{\left(\sum_i y_i\right)\left(\sum_i x_i\right)^2 - \left(\sum_i x_i\right)\left(\sum_i y_i x_i\right)}{N\sum_i x_i^2 - \left(\sum_i x_i\right)^2}$$

(21)

which successfully regains the noise term that is otherwise consecrated by means of a variational statistical (optimization of errors' squares summation) procedure.

With this description, it is clear that the SPECTRAL-SAR methodology not only recovers the standard statistical QSAR least square correlation results but also *generalizes* it analytically to a great extent toward a better assessment of mechanistically ordering and influences in practical eco- and bio- logical applications.

4. From in Cerebro to in Silico Principles of Ecotoxicity

When utilizing the analytical model of QSAR/Spectral-SAR for environmental interactions, one should consider the framework of the principles both at the general and applied levels. As such, regarding the general principles or green chemistry and engineering, they are provided in Table 2 to ensure that they can be readily compared [88]. Note that the fundamental principles constitute the background or the general framework or desiderate that is eventually supported by the associate engineering principle; the green engineering principle is primarily based on "minimizing" or "maximizing" the time, space, energy and costs, and it is constituted either in an economical enterprise and an extension of the main principles of nature or in terms of optimizing mass-energy and time-space. From this point forward, the most basic physical and chemical principles are observed as those acting on each process, system, or state to be created, maintained or modified [89-91].

However, while restraining the analysis to the specific interactions between chemical structures and biological species, the Organization for Economic Co-operation and Development (OECD) advanced a set of standard principles for the validation and for regulatory purposes of the (quantitative) structure-activity relationship models [92-95]:

- QSAR-1: a defined endpoint

- QSAR-2: an unambiguous algorithm

- QSAR-3: a defined domain of applicability

- QSAR-4: appropriate measures of goodness-of–fit, robustness and predictivity

• QSAR-5: a mechanistic interpretation, if possible

No.	Principle of Green Chemistry	Principle of Green Engineering
1.	Prevention of waste that must cleaned afterwards	Prevention rather than treatment
2.	Inherently safer chemistry for accident prevention such as releasing, explosions, and fires	Inherent rather than circumstantial processes and components to prevent hazard
3.	Atom economy in maximizing the incorporation of all material used	Conserving complexity of embedded entropy for minimizing the recycling process
4.	Less hazardous chemical systems should be designed with little or no toxicity	Design for commercial "afterlife" through their nontoxic availability
5.	Designing safer chemicals to minimize their toxicity	Durability rather than immortality because whatever compound should be degradable
6.	Safer solvents and auxiliars (separation agents)	Integrate material and energy flows allowing interconnectivity in components
7.	Designing for energy efficiency while synthetic methods should be conducted at ambient temperature and pressure whenever possible.	Maximizing efficiency in producing products through minimizing mass, energy, space, and time consumption
8.	Use of renewable raw materials and feedstocks rather than depleting them	Design for separation and purification operations should maximize recycling
9.	Reducing derivatives as those modifying physical-chemical processes because they are virtually converted into waste	Minimizing material diversity in multicomponent products towards promoting easiest disassembly process
10.	The use of catalytic rather than stoichiometric reagents is desirable for maintaining control over the selectivity	Output-pulled of reaction products rather than input-pushed reactants as additional starting material
11.	Design for degradation targeting biodegradability and not persistent components in environment	Renewable rather than depleting of material and energy inputs
12.	Real time analysis for pollution prevention by means of in-process monitoring and analytical methodologies	Meet need while minimizing the excess of unnecessary capacities or capabilities for bio-physicochemical systems

Table 2. The twelve principles of Green Chemistry and Engineering [89-91].

Within this context, the present QSAR-Spectra-SAR (QSAR-SSAR) approach "responds" to these OECD-QSAR principles by the present Spectral-SAR ecotoxicological principles' realization [96], with special reference to ionic liquids (Principle 3):

• *ECOTOX-SSAR Principle 1 is assured by:* the "length" of the predicted/measured (eco)biological action follows the self-scalar product rule of the computed endpoint activity

$$\left\| Y \right\rangle^{ENDPOINT\,(MEASURED/PREDICTED)} \Big\| = \sqrt{\sum_{i=1}^{N}\left(y_i^2\right)^{MEASURED/PREDICTED}} \tag{22}$$

- *ECOTOX-SSAR Principle 2 is assured by:* the "orthogonality" of assumed molecular factors that correlate with eco- and bio-effects is assured by the spectral decomposition of the associate activity respecting them (see eq. (8)), and the orthogonal-real space transformation given by the Spectral-determinant, eq. (11), giving in fact the searched structure-activity relationship model;

- *ECOTOX-SSAR Principle 3 is assured by:* the method of considering the structural parameters and the activities with which they should be correlated, for specific (target) class of molecules; for instance, the consecrated Hansch quantitative structure activity relationships (QSARs) generally prescribes the activity expansion under the generic minimal but meaningful form:

$$A = B_0 + B_1\left(\begin{array}{c}electronic\\parameter\end{array}\right) + B_2\left(\begin{array}{c}hydrophobic\\parameter\end{array}\right) + B_3\left(\begin{array}{c}steric\\parameter\end{array}\right) \tag{23}$$

which provides sufficient information about the transport, electronic affinity and specific interaction at the molecular level, respectively; whereas the hydrophobicity index, *LogP*, describes, at best, the quality of molecular transport through cellular membranes. For the electronic and steric contributions, many structural parameters may be considered [97,98]; among them, the polarizability (*POL*) measures the inductive electronic effect that reflects the long range or van der Waals bonding, whereas for the steric component, the total energy (E_{TOT}) is assumed to be the representative index because it is calculated at the optimum molecular geometry at which the stereo-specificity is included. These parameters have been demonstrated to be quite reliable in modeling the ecotoxicological interactions [26, 29, 30], and they will also be used in the present IL applications. To this aim, when information about the eco-biological influence of ionic liquids (*IL*) is desired, the particular anionic-cationic structure has to be properly considered because almost all structural information about ionic liquids is based on the superposition of the separate anionic and cationic contributions. In this situation, two different additive models for modeling anionic-cationic interaction can be considered. The *first* model is based on the vectorial summation of the produced anionic and cationic biological effects. In other words, this so-called |1+> model is constructed from the superposition of the anionic (subscripted with *A*) and cationic (subscripted with *C*) activities, and can be formally represented as [27, 30]:

$$\left|Y_{AC}\right\rangle^{1+} = \left|1+\right\rangle = \left|Y_A\right\rangle + \left|Y_C\right\rangle = \hat{O}_{S-SAR}\left[g\left(\left\{\left|X_A\right\rangle\right\}\right) + g\left(\left\{\left|X_C\right\rangle\right\}\right)\right] \tag{24}$$

with Hansch combinations

$$\left\{\left|X_{A,C}\right\rangle\right\} = \left\{LogP_{A,C}, POL_{A,C}, E_{TOT(A,C)}\right\} \tag{25}$$

Practically, with the $|1+\rangle$ model, the SPECTRAL-SAR procedure is separately performed for the anionic and cationic subsystems, and it is subsequently summed in the resulting *IL*-activity. The *second* SPECTRAL-SAR model can be advanced here when the additive stage is considered at the incipient stage of the SPECTRAL-SAR operator (1) such that the considered Hansch factors, for instance, are first combined to produce the anionic-cationic (subscripted with *AC*) indices that are further used to produce the spectral mechanistic map of the concerned interaction, producing the so-called $|0+\rangle$ model [28, 30]:

$$\left|Y_{AC}\right\rangle^{0+} = \hat{O}_{S-SAR}\left|0+\right\rangle = \hat{O}_{S-SAR} f\left(\left\{\left|X_A\right\rangle\right\}, \left\{\left|X_C\right\rangle\right\}\right) \tag{26}$$

with the Hansch specification of the spectral vectors:

$$f\left(LogP_A, LogP_C\right) \equiv LogP_{AC} = \log\left(e^{LogP_A} + e^{LogP_C}\right) \in \left\{\left|X_{1AC}\right\rangle\right\} \tag{27}$$

$$f\left(POL_A, POL_C\right) \equiv POL_{AC} = \left(POL_A^{1/3} + POL_C^{1/3}\right)^3 \in \left\{\left|X_{2AC}\right\rangle\right\}\left[\mathring{A}^3\right] \tag{28}$$

$$f\left(E_A, E_C\right) \equiv E_{AC} = E_A + E_C - 627.71\frac{q_A q_C}{POL_{AC}^{1/3}} \in \left\{\left|X_{3AC}\right\rangle\right\}\left[kcal/mol\right] \tag{29}$$
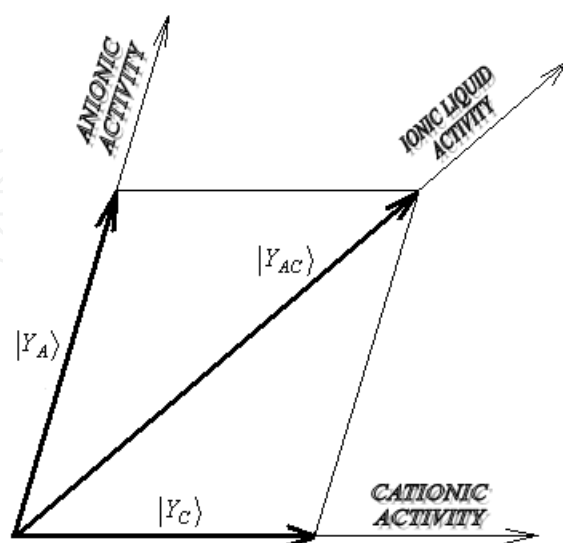

Figure 2. The vectorial composition of anionic and cationic sub-system activities in the ionic liquid global system, leading with the internal angle formation, with the trigonometric expression of eq. (30) [27,30].

The open issue addresses whether the $|0+\rangle$ & $|1+\rangle$ states leave with the same results or what aspects of the SPECTRAL-SAR operator (1) might differ in the *IL* ecotoxicity, a matter that is solved by computing the so-called *ionic liquid internal angle* between the anion-cationic activity vectors, Figure 2, with y_{iA}, y_{iC}, $i = \overline{1, N}$ components following the prescription [27,28,30,40]:

$$\cos\theta_{AC} = \frac{\langle Y_C | Y_A \rangle}{\|Y_C\rangle\| \|Y_A\rangle\|} = \frac{\displaystyle\sum_{i=1}^{N} y_{iC} y_{iA}}{\sqrt{\displaystyle\sum_{i=1}^{N} y_{iC}^2 \sum_{i=1}^{N} y_{iA}^2}} \begin{cases} \geq 0.707107 \ldots |0+\rangle \ MODEL \\ < 0.707107 \ldots |1+\rangle \ MODEL \end{cases} \tag{30}$$

- *ECOTOX-SSAR Principle 4 is assured by* the "intensity" of the chemical-eco-bio-interaction that is determined by the ratio of the expected to measured activity norms [26,29,69]

$$RA \equiv r_{S-SAR}^{ALGEBRAIC} = \sqrt{\frac{\displaystyle\sum_{i=1}^{N} y_{i-PRED}^2}{\displaystyle\sum_{i=1}^{N} y_{i-OBS}^2}} = \frac{\|Y_{PRED}\rangle\|}{\|Y_{OBS}\rangle\|} \leq 1 \tag{31}$$

as a counterpart of the classical statistical correlation factor [69,98,99]

$$R \equiv r_{QSAR}^{STATISTIC} = \sqrt{1 - \frac{\displaystyle\sum_{i=1}^{N} \left(y_{i-OBS} - y_{i-PRED}\right)^2}{\displaystyle\sum_{i=1}^{N} \left(y_{i-OBS} - \frac{1}{N}\displaystyle\sum_{i=1}^{N} y_{i-OBS}\right)^2}} \tag{32}$$

- *ECOTOX-SSAR Principle 5 is assured by* the "selection" of the manifested chemical-eco-(bio-)binding that parallels the minimum distances of paths [26,96,97]

$$\delta[A, B] = 0 \tag{33}$$

connecting all possible endpoints in the norm-correlation hyperspace

$$[A, B] = \sqrt{\left(\|Y_B\rangle\| - \|Y_A\rangle\|\right)^2 + \left(r_B^{STATISTIC/ ALGEBRAIC} - r_A^{STATISTIC/ ALGEBRAIC}\right)} \tag{34}$$

In this manner, the "validation" of the obtained mechanistic picture is achieved by requiring that the influential minimum paths are numbered by the cardinal of the input structural fac-

tors set such that, excepting that the final endpoint that is always considered as the final evolution target, all other endpoints are activated one time and one time only.

The present chapter reviews the presented Spectral-SAR-IL models as applied to studying the ecotoxicity of the aquatic species *Vibrio fischeri* and *Daphnia magna* by the tested ionic liquids, which were appropriately chosen such that they contained a wide variety of heads, side chains, and anions.

5. Two Cases of Ionic Liquids Ecotoxicity

Long and short term tests are used to explore the toxicity of the ionic liquids [100-102].

NAME	A_{exp} $\lvert Y_{EXP}\rangle$	Log P		Polarizability		TOTAL ENERGY	
		CAT. $\lvert X_{1C}\rangle$	AN. $\lvert X_{1A}\rangle$	CAT. $\lvert X_{2C}\rangle$	AN. $\lvert X_{2A}\rangle$	CAT. $\lvert X_{3C}\rangle$	AN. $\lvert X_{3A}\rangle$
1-n-butylpyridinium chloride	0.41*	2.85	0.63	17.51	2.32	-250008.14	-285190.78
1-n-butylpyridinium dicyanoamide	0.31*	2.85	0.43	17.51	5.51	-250008.14	-147935.98
1-n-butyl-3-methylpyridinium dicyanoamide	-0.34*	3.32	0.43	19.35	5.51	-274222.62	-147935.98
1-n-butyl-3,5-dimethylpyridinium dicyanoamide	-0.62*	3.78	0.43	21.18	5.51	-298437.03	-147935.98
1-n-butylpyridinium bromide	0.40*	2.85	0.94	17.51	3.01	-250008.14	-1596918.25
1-n-butyl-3-methylpyridinium bromide	-0.25*	3.32	0.94	19.35	3.01	-274222.62	-1596918.25
1-n-butyl-3,5-dimethylpyridinium bromide	-0.31*	3.78	0.94	21.18	3.01	-298437.03	-1596918.25
1-n-hexyl-3-methylpyridinium bromide	-0.94*	4.11	0.94	23.02	3.01	-322641.81	-1596918.25
1-n-octyl-3-methylpyridinium bromide	-2.21*	4.90	0.94	26.69	3.01	-371060.81	-1596918.25

NAME	A_{exp} $\lvert Y_{EXP}\rangle$	Log P		Polarizability		TOTAL ENERGY	
		CAT. $\lvert X_{1C}\rangle$	AN. $\lvert X_{1A}\rangle$	CAT. $\lvert X_{2C}\rangle$	AN. $\lvert X_{2A}\rangle$	CAT. $\lvert X_{3C}\rangle$	AN. $\lvert X_{3A}\rangle$
1-n-butyl-4-dimethylaminopyridinium bromide	-0.68	3.11	0.94	22.53	3.01	-332525.97	-1596918.25
1-n-butyl-3-methylimidazolium dicyanoamide	0.67*	0.68	0.43	17.22	5.51	-260646.64	-147935.98
1-n-butyl-3-methylimidazolium chloride	0.71*	0.68	0.63	17.22	2.32	-260646.64	-285190.78
1-n-butyl-3-methylimidazolium bromide	1.01*	0.68	0.94	17.22	3.01	-260646.64	-1596918.25
1-n-butyl-3-methylimidazolium bis(trifluoromethanesulfonyl)imide	0.39	0.68	3.05	17.22	7.20	-260646.64	-1128283.62
1-n-hexyl-3-methylimidazolium bromide	-1.58*	1.47	0.94	20.89	3.01	-309065.84	-1596918.25
1-n-octyl-3-methylimidazolium bromide	-2.37*	2.26	0.94	24.56	3.01	-357484.59	-1596918.25
tetrabutylammonium bromide	0.27	4.51	0.94	30.91	3.01	-422421.97	-1596918.25
hexyltriethylammonium bromide	-0.54	2.71	0.94	23.57	3.01	-325587.25	-1596918.25
tetrabutylphosphonium bromide	-0.29	2.89	0.94	30.91	3.01	-600149.62	-1596918.25
tributylethylphosphonium diethylphosphate	0.07	2.02	2.63	27.24	10.53	-551729.87	-494172.37
Trihexyl(tetradecyl)phosphoniumbromide	0.41	9.23	0.94	60.27	3.01	-987499.25	-1596918.25
Cholinebis(trifluoromethanesulfonyl)imide	1.15	-0.76	3.05	11.36	7.20	-202450.36	-1128283.62

Table 3. The series of ionic liquids whose toxic activities A= Log(EC_{50}) on *Vibrio fischeri* were considered [49], with the marked values being taken from [45] along with the structural parameters *LogP*, *POL* (Å^3), and E_{TOT} (kcal/mol) that account for the hydrophobicity, electronic (polarizability) and steric (total energy at optimized 3D geometry) effects, computed with the help of the HyperChem program [103], for each cation and anion containing ionic liquid, respectively [27].

The results from using the Ames test for mutagenity with the *Salmonella typhyimurium* species indicated that none of the imidazolium, pyridinium and quaternary ammonium ionic liquids caused mutations. However, the Ames test is a short-term test, and it cannot be possible to fully predict the carcinogenicity in animals [46]. The antimicrobial activity (against strains of Gram-positive and –negative bacteria and fungi) increase with increasing alkyl chain lengths in pyridinium, imidazolium and quaternary ammonium salts [43]. However, because bacteria have a short generation time, they are an ideal starting point for investigating the structure-activity relationship in ionic liquids and serve as a basis for further toxicity tests to higher organisms and more complex systems; a few examples are listed below [45,67]:

- [BMIM][Br] (1-n-butyl-3-methylimidayolium bromide) was observed to be considerably less toxic than [BMPy][Br] (1-n-butyl-3-methylpyridinium bromide);

- Cation toxicity increases with the increase in the hydrophobicity of the molecules, from Bpy (1-n-butyl-3-pyridinium) to BMPy (1-n-butyl-3-methylpyridinium) to BdMPy (1-n-butyl-3-dimethylpyridinium);

- Butyl substituted ionic liquids have considerably lower logP values and are more water soluble;

- In comparison with some commonly used industrial solvents (acetone, methanol, ethyl acetate, and dichloromethane), the octyl and hexyl substituted ionic liquids are more toxic.

- [BMIM][Cl] (1-n-butyl-3-methylimidayolium bis(trifluoromethylsulfonyl)imide chloride) and [BPy][Cl] (1-n-butyl-3-pyridinium chloride) may have similar activity to the pesticide parquet.

Mode	Vectors (C/A/IL)	Cationic S-SAR			Anionic S-SAR			Ionic Liquid S-SAR		
		$\| \|Y_C)^{Mode}\|$	$r_{S-SAR}^{STATISTIC}$	$r_{S-SAR}^{ALGEBRAIC}$	$\| \|Y_A)^{Mode}\|$	$r_{S-SAR}^{STATISTIC}$	$r_{S-SAR}^{ALGEBRAIC}$	$\| \|Y_{AC})^{Mode}\|$	$r_{S-SAR}^{STATISTIC}$	$r_{S-SAR}^{ALGEBRAIC}$
Ia	$\|X_0\rangle, \|X_1\rangle$	1.47807	0.267342	0.334755	1.38453	0.238974	0.313569	2.58965	0.185959	0.586507
Ib	$\|X_0\rangle, \|X_2\rangle$	1.08531	0.132169	0.245803	1.48745	0.270118	0.33688	2.30825	0.179482	0.522776
Ic	$\|X_0\rangle, \|X_3\rangle$	0.9452	0.0469985	0.21407	1.75453	0.345553	0.397368	2.41575	0.259502	0.547123
IIa	$\|X_0\rangle, \|X_1\rangle, \|X_2\rangle$	1.64279	0.314715	0.372062	1.52849	0.282139	0.346174	2.88368	0.219986	0.653101
IIb	$\|X_0\rangle, \|X_1\rangle, \|X_3\rangle$	1.72651	0.3379	0.391023	2.15865	0.451919	0.488893	3.48056	0.352356	0.788283
IIc	$\|X_0\rangle, \|X_2\rangle, \|X_3\rangle$	1.71867	0.335748	0.389246	1.82903	0.365689	0.414242	3.17318	0.299925	0.718667
III	$\|X_0\rangle, \|X_1\rangle, \|X_2\rangle, \|X_3\rangle$	1.79053	0.355322	0.405522	2.36461	0.504184	0.53554	3.7151	0.397148	0.841402

Table 4. Spectral structure activity relationships (S-SAR) of the ionic liquids in Table 3 against their toxicity to *Vibrio fischeri*, and the associated computed spectral norms with $\| \|Y_{EXP}\rangle \|$ =4.41537, statistical and algebraic correlation factors, computed upon the relations (22), (31), and (32), throughout the possible correlation models considered from the *anionic, cationic and composed ionic liquids data* from Table 3, respectively [27]

Mode	Ia	Ib	Ic	IIa	IIb	IIc	III
$cos\theta_{AC}$	0.66397	0.600124	0.562018	0.653248	0.60019	0.599635	0.591015

Table 5. The variation of the cosines of the anion-cationic correlation angle in vectorial space based on Eq. (30) for all considered modes of action of the ionic liquids in Table 3 with the cationic and anionic subsystems S-SAR predicted activities, respectively [27].

Path	Value					
	Cationic		Anionic		Ionic Liquid	
	statistic	*algebraic*	*statistic*	*algebraic*	*statistic*	*algebraic*
Ia-IIa-III	0.324618	**0.320376 α**	1.0154	1.0049	1.14608	**1.15396 α**
Ia-IIb-III	0.324616	0.320376	**1.01536 γ**	**1.0049 γ**	**1.1451 α**	1.15396
Ia-IIc-III	**0.324616 α**	0.320376	1.01541	1.0049	1.14513	1.15396
Ib-IIa-III	0.739827	0.723082	**0.907864 β**	**0.899373 β**	**1.42694 γ**	1.44248
Ib-IIb-III	**0.739746 β**	0.723082	0.907871	0.899373	1.42377	**1.44248 γ**
Ib-IIc-III	0.739754	**0.723082 β**	0.907893	0.899373	1.42385	1.44248
Ic-IIa-III	**0.900418 γ**	0.86674	1.09986	1.08906	1.31968	1.33226
Ic-IIb-III	0.900057	**0.86674 γ**	0.630373	0.625533	1.30763	1.33226
Ic-IIc-III	0.90009	0.86674	**0.630371 α**	**0.625533 α**	**1.30908 β**	**1.33226 β**

Table 6. Synopsis of the statistic and algebraic values of paths connecting the S-SAR models of Table 4 in the norm-correlation spectral-space of eq. (34) for the ionic liquids in Table 3 against the toxicity to *Vibrio fischeri*. The primary, secondary and tertiary - the so called alpha (α), beta (β) and gamma (γ) paths - are indicated according to the least path principle in spectral norm-correlation space with the statistical and algebraic variants of the correlation factors used, respectively [27].

The Microtox Acute Toxicity Test is often used to determine the toxicity of single compounds in sediment contamination studies and for monitoring industrial effluents in environmental water quality surveys [49,100]. Before releasing the ionic liquids into the environment, the antimicrobial properties using *Vibrio fischeri* in the Microtox method were thoroughly examined [45]. Equally, by other tests with *Vibrio fisheri*, an increase in the toxicity corresponding to an increase in the chain length and an increase in the number of alkyl groups substituted on the cation ring was also demonstrated [45,101].

Salts used for anion substitution, such as sodium bromide and sodium dicyanoamide, were less toxic to *Vibrio fisheri* than the compounds used for synthesizing the cation. For instance, 3-methyl pyridine and 1-methylimidazole may be used as starting compounds. The addition of a butyl chain to the C1 (carbon atom) of the pyridinium and imidazolium cation slightly increased the toxicity of the ionic liquid. Furthermore, the addition of a hexyl or octyl chain will also increase the toxicity. The same observation holds for quaternary ammonium salts. All of these observations suggest that the effects are related to the lipophilicity of the cation, thus explaining why many of the imidazolium and pyridinium ionic liquids were more tox-

ic than acetonitrile, acetone and methanol. In contrast, monatomic anions (such as bromide, chloride) are predicted to be less toxic than large anions that contain regions of positive charge, e.g., TFMSi (bis(trifluoromethylsulfonyl)imide) [49].
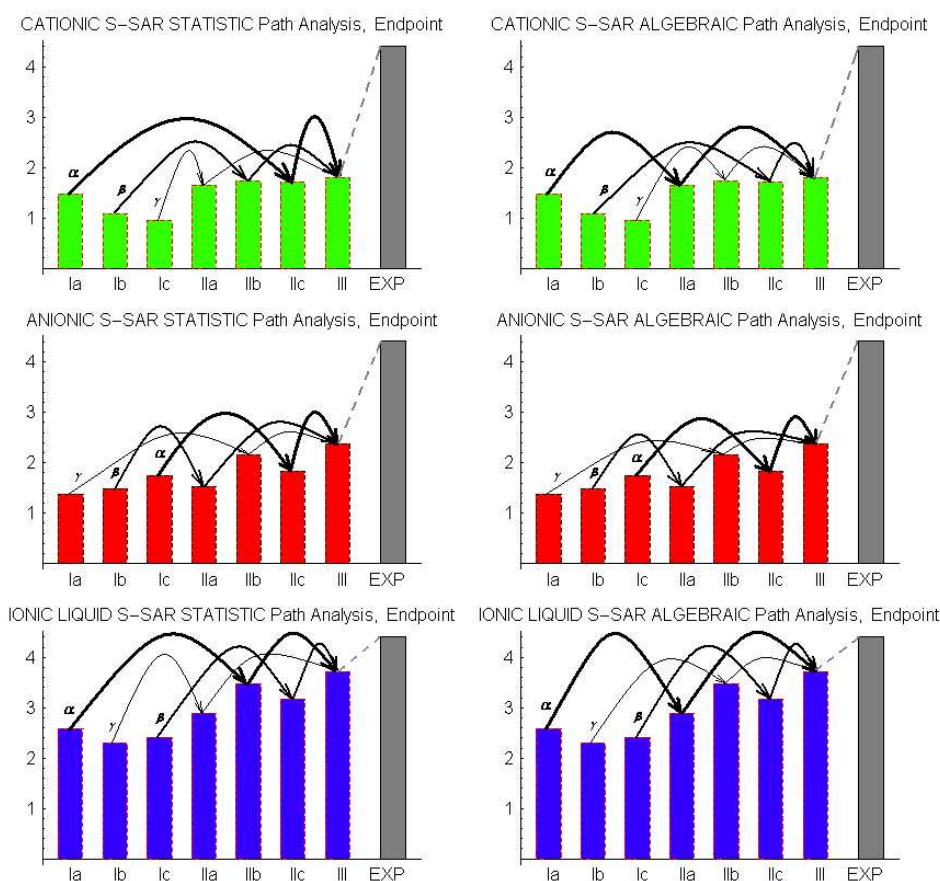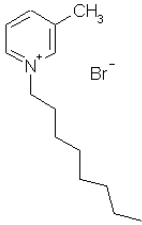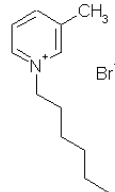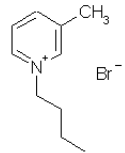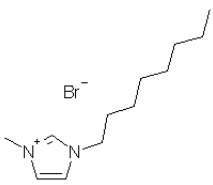

Figure 3. The spectral representation of the chemical-biological interaction paths across the S-SAR to the modeled endpoints of the *Vibrio fischeri*, according to the least (shortest) path rule within the spectral norm-correlation space applied to the data in Table 6 for the cationic, anionic and resulting ionic liquid norms of Table 4 for the statistical and algebraic versions of correlation factors from up to down and left to right, respectively. The primary-alpha, secondary-beta and tertiary-gamma path hierarchies of Table 6 are indicated by decreasing thicknesses of the connecting lines [27].
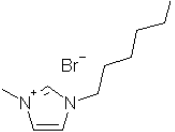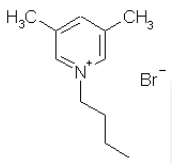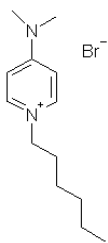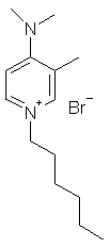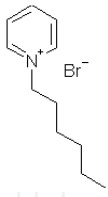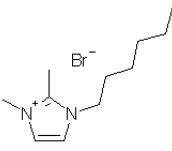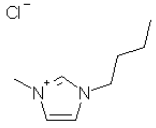
At the organism level, which are *Vibrio fisheri* and *Daphnia magna* in this review, the toxicity generally increases with the cation type as ammonium<pyridinium<imidazolium<triazoli-um<tetrazolium. The choline ionic liquids (with a negatively charged oxygen atom) and the quaternary ammonium ionic liquids with short chain lengths were relatively non-toxic to *Vibrio fisheri*. Furthermore, the methylation of the aromatic ring of the cation reduces the tox-icity to *Vibrio fisheri* and *Daphnia magna* [49]. The toxicity increases with the number of nitro-gen atoms, whereas the anions play a secondary role in the toxicity (even if the presence of positively charged atoms on the anion is predicted to slightly increase the toxicity) [49].

Note that *Daphnia* is an important link between the microbial and higher trophic levels [49,102]. By acting on *Daphnia magna*, ionic liquids with longer alkyl chain substituents have

toxicities comparable to phenol, whereas those with shorter substituents (for example, [BMIM][Br]) were more toxic to *Daphnia magna* than benzene and methanol [47,49].

The lethal concentration to *D. magna* (also called the acute toxicity) was observed to be considerably lower for ILs that employed imidazolium as cation than salts with Na^+; therefore, the toxicity was related to the imidazolium cation and not to the anions. With respect to the life history of the freshwater crustacean, salts with a sodium cation ($NaPF_6$ sodium hexafluorophosphate and $NaBF_4$, sodium tetrafluoroborate) affect the reproduction of *D. magna* at high concentrations. Sub-lethal effects on the life-history traits occurred when the concentrations of the ionic liquids were an order of magnitude lower than those for acute effects. The clonally variation was a possible reason why the average brood size in controls with those for ionic liquids. This was the first study on aquatic eukaryotes [47]. The EC50 values on the toxicity to a single species are necessary for further studies at the community and ecosystems levels [47]. Overall, qualitatively, the toxic effects were not observed to be notably different for the imidazolium and pyridinium ionic liquids, although the toxicity was greater with an increase in the length of the side chain. The K_{ow} values for the IL were lower than those of chemicals that bioaccumulate in the tissue of organisms. Quantitative analysis by the presented QSAR/Spectral-SAR algorithm follows.

Ionic Liquid Compound		A_{exp}	LogP			POL [Å³]			E_{TOT} [kcal/mol]		
Structure	*Name*	$|Y_{exp}>$	$|X_{1C}>$	$|X_{1A}>$	$|X_{1AC}>$	$|X_{2C}>$	$|X_{2A}>$	$|X_{2AC}>$	$|X_{3C}>$	$|X_{3A}>$	$|X_{3AC}>$
	1-n-octyl-3-methylpyridinium bromide	-2.60	4.90	0.94	4.92	26.69	3.01	87.08	-371060.81	-1596918.25	-1967840
	1-n-hexyl-3-methylpyridinium bromide	-2.41	4.11	0.94	4.15	23.02	3.01	78.87	-322641.81	-1596918.25	-1919410
	1-n-butyl-3-methylpyridinium bromide	-1.24	3.32	0.94	3.41	19.35	3.01	70.37	-274222.62	-1596918.25	-1870990
	1-n-octyl-3-methylimidazolium bromide	-4.33	2.26	0.94	2.5	24.56	3.01	82.35	-357484.59	-1596918.25	-1954260

Ionic Liquid Compound	A_{exp}		LogP		POL [Å³]			E_{TOT} [kcal/mol]	
1-n-hexyl-3-methylimidazolium bromide	-2.22	1.47	0.94	1.93	20.89	3.01	73.98	-309065.84	-1596918.25	-1905830
1-n-butyl-3,5-dimethylpyridinium bromide	-1.01	3.78	0.94	3.84	21.18	3.01	74.65	-298437.03	-1596918.25	-1895210
1-n-hexyl-4-piperidino pyridinium bromide	-3.66	4.63	0.94	4.65	30.93	3.01	96.25	-452857.03	-1596918.25	-2049640
1-n-hexyl-4-dimethylamino pyridinium bromide	-3.28	3.91	0.94	3.96	26.2	3.01	86.00	-380945.12	-1596918.25	-1977720
1-n-hexyl-3-methyl-4-dimethylamino pyridinium bromide	-2.79	4.37	0.94	4.40	28.04	3.01	90.03	-405145.97	-1596918.25	-2001920
1-n-hexylpyridinium bromide	-1.93	3.64	0.94	3.71	21.18	3.01	74.65	-298427.37	-1596918.25	-1895200
1-n-hexyl-2,3-dimethylimidazolium bromide	-2.19	1.67	0.94	2.06	22.72	3.01	78.19	-333284.94	-1596918.25	-1930060
1-n-butyl-3-methylimidazolium chloride	-1.07	0.68	0.63 *	1.34	17.22	2.32	59.60	-260646.64	-285190.78	-545677
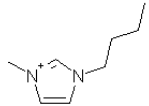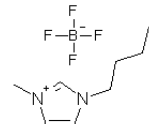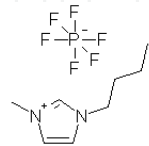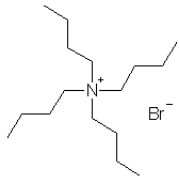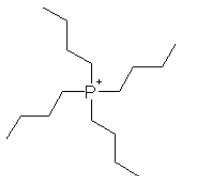
Ionic Liquid Compound	A_{exp}	LogP			POL [Å³]			E_{TOT} [kcal/mol]		
Br⁻ 1-n-butyl-3-methylimidazolium * bromide	-1.43	0.68	0.94	1.51	17.22	3.01	65.26	-260646.64	-1596918.25	-1857410
1-n-butyl-3-methylimidazolium * tetrafluoroborate	-1.32	0.68	1.37	1.78	17.22	2.46	60.80	-260646.64	-261310.59	-521798
1-n-butyl-3-methylimidazolium * hexafluorophosphate	-1.15	0.68	2.06	2.28	17.22	1.78	54.62	-260646.64	-580264.94	-840746
Tetrabutyl ammonium bromide	-1.53	4.51	0.94	4.54	30.91	3.01	96.21	-422421.97	-1596918.25	-2019200
Tetrabutyl phosphonium bromide	-2.05	2.89	0.94	3.02	30.91	3.01	96.21	-600149.625	-1596918.25	-2196930

Table 7. The actions of the studied ionic liquids on the *Daphnia magna* species with the toxic activities Aexp= Log(EC50) [49], while the marked values were taken from [47] along with the structural parameters LogP, POL, and ETOT to account for the hydrophobicity, electronic (polarizability) and steric (total energy at optimized 3D geometry) effects, computed with the HyperChem program [103], for each cation and anion fragment, and for the anionic-cationic |0+> composed state by means of equations (27)-(29), respectively [28].

The application of S-SAR-IL to *Vibrio Fischeri* conforms with the |1+> model presented above for the data presented in Table 3. Accordingly, the Spectral-SAR models for anions and cations are reported in Table 4, and the internal angle for all of the possible models are listed in Table 5, which confirms that model |1+>, with the results at the global level of ionic liquids being shown on the last column of Table 4.

Picturing a mechanistically mode of action for ionic liquids containing cations and anions and of their summed effects on the considered *Vibrio fischeri* species remains as the final purpose of the QSAR method, OECD-QSAR normative, and the Spectral-SAR algorithm, as extensively presented. In this regard, the spectral paths analysis is presented in Table 6, which is based on eqs. (33) and (34) with the cationic, anionic and ionic liquids data of Table 4. The minimum path procedure assumes the identification of the minimum paths (equal in numbers with the number of structural parameters considered, thus *alpha*, *beta*, and *gamma* for the present case), in an "ergodic manner"; this means that the overall path is firstly identi-

fied; if two or more paths appear with equal lengths, the one to be chosen is the one that contains the "minimum first movement", which is that path that links the closest first two norms that belong to successive norms; therefore, the second overall minimum path is identified such that it does not contain the models "touched" by the *alpha* path, thereby excluding the common final endpoint (model III here). In this manner, the remaining *beta* and *gamma* paths are also selected. Such analysis is performed for both statistical and algebraic norms; see Table 6. In this manner, interesting results are obtained, allowing conceptual interpretation, such as the following [27]:

- While in cationic case, the statistical and algebraic paths do not coincide (e.g., what the alpha *Ia-IIc-III* path in statistic differs than the alpha *Ia-IIa-III* path in algebraic views), in the anionic case, they are identically predicted (except the fact that in the algebraic case, the shortened paths are registered), which together provide a mixed behavior for the resulting ionic liquid (only the beta path *Ic-IIc-III* is overlapping between statistical and algebraic views);

- While in the cationic and anionic subsystems, the path hierarchies are reversed as $\alpha \rightarrow \beta \rightarrow \gamma$ and $\gamma \rightarrow \beta \rightarrow \alpha$. In the resulting ionic liquid, the mixture effect is again observed because the succession $\alpha \rightarrow \gamma \rightarrow \beta$ against the successions of starting endpoints $Ia \rightarrow Ib \rightarrow Ic$, respectively;

- The cationic alpha path is started on the lipophylicity causes (*Ia*), which is the same as for the containing ionic liquid. A different situation arises for the alpha anionic path that begins with the steric influence (*Ic*); in this way, the previously noted dominance of the cationic influence when correlated with lipophilicity and the observed anionic influence related with steric effects are theoretically confirmed in this picture;

- Figure 3 clearly illustrates the fact that while anionic and cationic activity tendencies are somewhat complementary, they do not cancel each other in the ionic liquid that contains them but add up to attain the overall observed toxicity, in the spectral norm – correlation factor space. Furthermore, other useful data can be extracted from Figure 3 concerning the major path of structural causes in manifested toxicological action, as revealed below;

- While the algebraic paths are systematically lower that the corresponding statistical ones for cationic and anionic subsystems, in the ionic liquid case, the situation is reversed; the interpretation is that it also confirms that the chemical-biological ionic liquid dispersive (not specific) actions in environment are merely through its subsystem components than from itself as a whole;

- The ecotoxicological paths in the cationic and anionic subsystems are summed up in the paths of the corresponding ionic liquids in a nontrivial manner: the anionic gamma path effect is marginal over the cationic alpha path

$$\alpha_C + \gamma_A = \alpha_{AC} \qquad (35)$$

- the cationic and anionic beta paths decay into the gamma ionic liquid path when joined such that recording a sort of reciprocal cancellation of their effects

$$\beta_C + \beta_A = \gamma_{AC} \tag{36}$$

- the anionic alpha path effect is reinforced over the cationic gamma path averaging both at the beta path level of the resulting ionic liquid

$$\gamma_C + \alpha_A = \beta_{AC} \tag{37}$$

Mode	Vectors' Predicted	$\||Y\rangle^{Mode}\|$	$r_{S-SAR}^{STATISTIC}$	$r_{S-SAR}^{ALGEBRAIC}$
Ia	$|Y_{A-Ia}\rangle = f(|X_0\rangle,|X_{1A}\rangle)$	8.83127	0.266552	0.920421
	$|Y_{C-Ia}\rangle = f(|X_0\rangle,|X_{1C}\rangle)$	8.92169	0.420761	0.929845
	$|Y_{AC-Ia}\rangle^{0+} = f(|X_0\rangle,|X_{1AC}\rangle)$	8.89048	0.374616	0.926593
	$|Y_{AC-Ia}\rangle^{1+} = |Y_{A-Ia}\rangle + |Y_{C-Ia}\rangle$	17.6883	2.21964 *i*	1.84353
Ib	$|Y_{A-Ib}\rangle = f(|X_0\rangle,|X_{2A}\rangle)$	8.94784	0.455964	0.932572
	$|Y_{C-Ib}\rangle = f(|X_0\rangle,|X_{2C}\rangle)$	9.06691	0.59121	0.944981
	$|Y_{AC-Ib}\rangle^{0+} = f(|X_0\rangle,|X_{2AC}\rangle)$	*9.08979*	*0.613973*	*0.947366*
	$|Y_{AC-Ib}\rangle^{1+} = |Y_{A-Ib}\rangle + |Y_{C-Ib}\rangle$	17.9079	2.19638 *i*	1.86641
Ic	$|Y_{A-Ic}\rangle = f(|X_0\rangle,|X_{3A}\rangle)$	8.96309	0.475327	0.934161
	$|Y_{C-Ic}\rangle = f(|X_0\rangle,|X_{3C}\rangle)$	8.95817	0.469161	0.933648
	$|Y_{AC-Ic}\rangle^{0+} = f(|X_0\rangle,|X_{3AC}\rangle)$	*8.99267*	*0.510889*	*0.937244*
	$|Y_{AC-Ic}\rangle^{1+} = |Y_{A-Ic}\rangle + |Y_{C-Ic}\rangle$	17.8233	2.20167 *i*	1.8576
IIa	$|Y_{A-IIa}\rangle = f(|X_0\rangle,|X_{1A}\rangle,|X_{2A}\rangle)$	8.96021	0.47173	0.933861
	$|Y_{C-IIa}\rangle = f(|X_0\rangle,|X_{1C}\rangle,|X_{2C}\rangle)$	9.06885	0.59317	0.945183
	$|Y_{AC-IIa}\rangle^{0+} = f(|X_0\rangle,|X_{1AC}\rangle,|X_{2AC}\rangle)$	*9.1014*	*0.62522*	*0.948575*
	$|Y_{AC-IIa}\rangle^{1+} = |Y_{A-IIa}\rangle + |Y_{C-IIa}\rangle$	17.9161	2.1931 *i*	1.86727
IIb	$|Y_{A-IIb}\rangle = f(|X_0\rangle,|X_{1A}\rangle,|X_{3A}\rangle)$	8.96426	0.476781	0.934283
	$|Y_{C-IIb}\rangle = f(|X_0\rangle,|X_{1C}\rangle,|X_{3C}\rangle)$	8.99112	0.50908	0.937082
	$|Y_{AC-IIb}\rangle^{0+} = f(|X_0\rangle,|X_{1AC}\rangle,|X_{3AC}\rangle)$	*8.99774*	*0.51675*	*0.937772*
	$|Y_{AC-IIb}\rangle^{1+} = |Y_{A-IIb}\rangle + |Y_{C-IIb}\rangle$	17.8793	2.21324 *i*	1.86343
IIc	$|Y_{A-IIc}\rangle = f(|X_0\rangle,|X_{2A}\rangle,|X_{3A}\rangle)$	8.96808	0.481497	0.93468
	$|Y_{C-IIc}\rangle = f(|X_0\rangle,|X_{2C}\rangle,|X_{3C}\rangle)$	9.09155	0.615686	0.947549
	$|Y_{AC-IIc}\rangle^{0+} = f(|X_0\rangle,|X_{2AC}\rangle,|X_{3AC}\rangle)$	9.09116	0.615307	0.947508
	$|Y_{AC-IIc}\rangle^{1+} = |Y_{A-IIc}\rangle + |Y_{C-IIc}\rangle$	17.9586	2.19937 *i*	1.8717

Mode	Vectors' Predicted	$\| \|Y\rangle^{Mode}\|$	$r_{S-SAR}^{STATISTIC}$	$r_{S-SAR}^{ALGEBRAIC}$
III	$\|Y_{A\text{-}III}\rangle = f(\|X_0\rangle,\|X_{1A}\rangle,\|X_{2A}\rangle,\|X_{3A}\rangle)$	8.96926	0.482946	0.934803
	$\|Y_{C\text{-}III}\rangle = f(\|X_0\rangle,\|X_{1C}\rangle,\|X_{2C}\rangle,\|X_{3C}\rangle)$	9.12145	0.644232	0.950666
	$\|Y_{AC\text{-}III}\rangle^{0+} = f(\|X_0\rangle,\|X_{1AC}\rangle,\|X_{2AC}\rangle,\|X_{3AC}\rangle)$	9.10319	0.62694	0.948762
	$\|Y_{AC\text{-}III}\rangle^{1+} = \|Y_{A\text{-}III}\rangle + \|Y_{C\text{-}III}\rangle$	17.9531	2.17933 i	1.87113

Table 8. Spectral structure activity relationships (SPECTRAL-SAR) of the ionic liquids toxicity of Table 7 against the *Daphnia magna* species, and the associated computed spectral norms, with $\| \|YEXP\rangle \| = 9.59481$, statistic and algebraic correlation factors [26,30], throughout the possible correlation models considered from the anionic, cationic, and ionic liquid |1+> and |0+> states, respectively [28].

Mode	Ia	Ib	Ic	IIa	IIb	IIc	III
$cos\theta_{AC}$	0.985468	0.976338	0.978196	0.975018	0.983081	0.97768	0.969683

Table 9. The values of the cosines of the anion-cationic vectorial angles [27,30] for all considered modes of action of Table 8 indicating the |0+> states of the considered ionic liquids [28].

Path	Cationic		Anionic		Ionic Liquid			
					state |0+>		state |1+>	
	statistic	algebraic	statistic	algebraic	statistic	algebraic	statistic	Algebraic
Ia-IIa-III	0.299988	0.200851	**0.256742γ**	0.13874	0.330033	**0.213862 γ**	0.260535	0.266181
Ia-IIb-III	**0.300103γ**	0.200851	0.2567	0.13874	**0.330581 γ**	0.213862	**0.25639γ**	**0.266181γ**
Ia-IIc-III	0.299895	**0.200851 γ**	0.25666	**0.13874 γ**	0.33011	0.213862	0.269477+ R* i	0.277223
Ib-IIa-III	**0.07607α**	**0.0548409 α**	0.034447	**0.0215298 β**	0.0186427	0.0134673	**0.0418672 α**	**0.0454552α**
Ib-IIb-III	0.299514	0.207241	0.0344468	0.0215298	0.286398	0.198562	0.0886683	0.102966
Ib-IIc-III	0.0760732	0.0548409	**0.0344464β**	0.0215298	**0.0186427 α**	**0.0134673 α**	0.0506137+ R* i	0.0564973
Ic-IIa-III	0.23953	0.16417	0.0190146	0.0119873	**0.160257 β**	0.111113	0.126723	0.130484
Ic-IIb-III	0.23952	**0.16417 β**	**0.00980164 α**	**0.00619966α**	0.160264	**0.111113 β**	**0.120323 β**	**0.130484β**
Ic-IIc-III	**0.239484 β**	0.16417	0.00980164	0.00619966	0.16027	0.111113	0.135252+ R* i	0.141526

Table 10. Synopsis of the statistical and algebraic values of the paths connecting the SPECTRAL-SAR models of Table 8, in the norm-correlation spectral-space, for *Daphnia magna* species against the ionic liquids toxicity of Table 7; the primary, secondary and tertiary - the so called alpha (α), beta (β) and gamma (γ) paths, are indicated according to the "selection" and "validation" principles in norm-correlation spectral space when the statistic and algebraic variants of the correlation factors are respectively used [28].
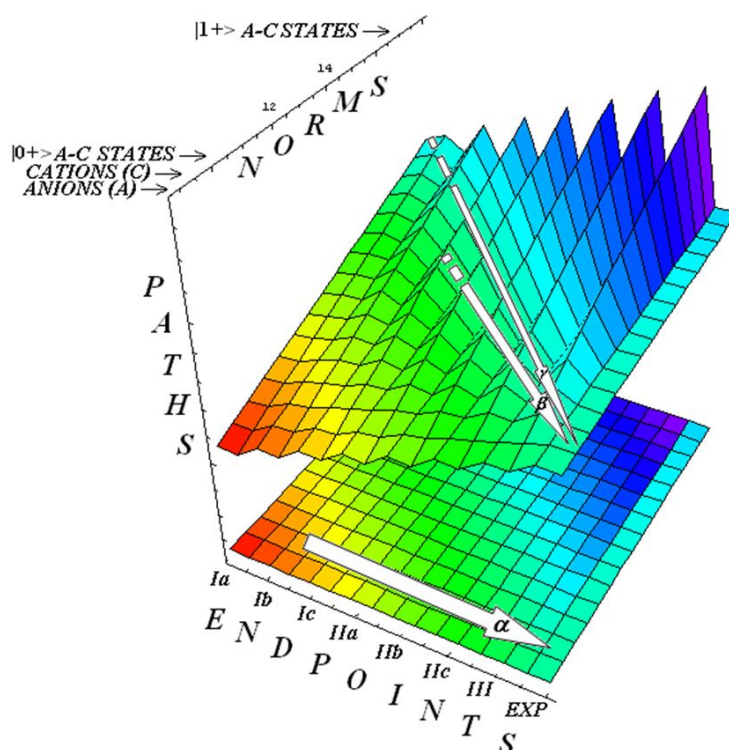
Figure 4. The spectral hypersurface of the structural hierarchical paths toward the recorded (*EXP*) ecotoxicological activity (in the extreme right hypersurface region) of the ionic liquids of Table 7 on *Daphnia magna* species: the alpha path (*α*) initiates on the polarizability (*Ib*) anionic-cationic interaction (in the left-bottom hypersurface region), being followed by the beta path (*β*), which originates on the steric (*Ic*) anionic-cationic interaction (in the left-top hypersurface region hypersurface region), and successively by the gamma path (*γ*) based on the hydrophobic (*Ia*) anionic-cationic interaction (in the extreme left-top hypersurface region) of the norm-correlation spectral space of Table 8 with the decaying order of the thickness of the connecting arrows, respectively [28].

When turning to the study of the action of ionic liquids on the *Daphnia* species, the pool of molecules in Table 7 are employed for assessing the SAR-Ionic Liquid Ecotoxicological $|0+>$ Model for IL-*Daphnia* chemical-biological interaction. This fact is confirmed by employing eqs. (27)-(29) for the cationic and anionic data of Table 7 and later computing the S-SAR determinants (11) associated with all models and combinations presented in Table 8, which leads to the internal angle computations and the results in Table 9 and assures the application of the model $|0+>$ is in accordance with the prescription given by eq. (30). Within the Spectral-SAR algorithm and allied eco-toxicological principles, the results allow the specific conclusions [28]:

- From the toxicological actions of Table 8, it can be observed that both anionic and cationic fragments have important contributions to the "length" and "intensity" of the ionic liquids ecotoxicity through the computed spectral norms and algebraic correlation factors, respectively, which are close to the experimental one, i.e., to 9.59481;

- In all cases, the mode of action where all three Hansch factors were considered (mode *III* with *LogP+POL+E $_{TOT}$*) records the best norm and correlations that are the closest description of the ionic liquids-*Daphnia magna* chemical-biological interaction;

- The cationic influence is observed with the dominant contribution over the anionic effects in ecotoxicity, in all considered Hansch modes of action;

- The statistical correlation factors always yield smaller values than the corresponding algebraically ones, see Table 8;

- There are recorded imaginary statistical correlations of the computed endpoints $|Y_{AC-Mode}>^{1+}$ that indicate certain limitations of its use for activity modeling in ecotoxicology; for these cases, the algebraically outputs provide almost the sum of the anionic and cationic length and intensity endpoint activity. This result can be phenomenologically explained by the so-called "resonance effect" when the angles between the anionic and cationic endpoint vectors are almost zero, as clearly evidenced by the cosine values of Table 9;

- Within the $|0+>$ model, all of the lengths and intensities of the endpoints $|Y_{AC-Mode}>^{0+}$ behave as an average of the anionic and cationic ecotoxicological effects with a smooth increase over the individual cationic effects for the modes *Ib* (POL), *Ic* (E $_{TOT}$), *IIa* (*LogP* +POL), and *IIb* (*LogP*+E $_{TOT}$); however, further selection for the binding mechanism is performed by identifying the minimum analysis of the Spectral-paths, Table 10.

The Spectral path analysis is unfolded in the same manner as previously used for the $|1+>$ models, i.e., by "ergodic" selection of the models per paths, with the ecotoxicological results in Table 10 and correspondingly interpreted as follows [28]:

- the additive parametric and endpoint models, $|0+>$ and $|1+>$, provide the same hierarchies of the paths for the chemical-biological actions;

- the statistical imaginary correlation values for the ionic liquids $|1+>$ are avoided from the mechanistic principle and do not belong to any selected path in Table 10;

- the dominant cationic effects can also be noted here at the least paths level because the nature of the cationic mechanism is preserved to the ionic liquids nature according with the spectral path equations:

$$\alpha_C + \beta_A = \alpha_{IL} \tag{38}$$

$$\beta_C + \alpha_A = \beta_{IL} \tag{39}$$

$$\gamma_C + \gamma_A = \gamma_{IL} \tag{40}$$

- the results of all SPECTRAL-SAR ecotoxicological principles applied to ionic liquids-*Daphnia magna* case of chemical-eco-biological interaction can be unitarily presented in the Figure 4, where the spectral hypersurface was generated by the 3D interpolation of all lengths (norms) for all the endpoint modes of Table 8, for all cationic, anionic, $|0+>$ and $|1+>$ states of ionic liquids of Table 7. The alpha dominant paths are easily identified according to Table 10, as originating in the *Ib*, i.e., on *POL*arizability or van der Waals mo-

lecular mode of action, while the beta and gamma ones starts with the steric (*Ic*: E_{TOT}) and hydrophobic (*Ia*: *Log*P) specific chemical-biological binding, respectively.

Overall, one may assess the sets of eqs. (35)-(37) and (38)-(40) as specific for ionic liquids action over biological marine species within the additive and parametric models |1+> and |0+>, respectively, that should be further confirmed or extended by future studies with other structural parameters (beyond Hansch descriptors, i.e., by topological and quantum molecular factors) and/or with other species on similar congeneric ILs and working algebraic chemical-biological interaction models.

6. Conclusions

Since their emergence a decade ago, ionic liquids (ILs) have had a constantly increasing influence on organic, bio- and green chemistry, due to their unique physico-chemical properties manifested by their typical salt structure: a heterocyclic nitrogen-containing organic cation (in general) and an inorganic or organic anion [43] with melting points below 100 ºC and no vapor pressure [47]. The latter property leads to the practical replacement of conventional volatile organic compounds (VOCs) from the point of view of atmospheric emissions, though they do present the serious drawback that a small amount of IL could enter the environment through groundwater [104]. This risk makes it necessary to perform further eco-toxicological studies of IL on various species to improve the "design rules" for synthesized ILs with minimal toxicity to the environmental integrated organisms. Ionic liquids display variable stability in terms of moisture and solubility in water, polar and nonpolar organic solvents [45]. Various values of ionic liquid hydrophobicity and polarity may be tailored [104] with the help of nucleoside chemistry [105] according to the main principles of green chemistry [54,66]: the new chemicals must be designed to preserve effectiveness of function while reducing toxicity and not persisting in the environment at the end of their usage but rather breaking down into inoffensive degradation products.

In this respect, the costs of all approaches for sustainable product design can be reduced using the SAR and QSAR methods [26-30]. While the 1-octanol-water partition coefficient could be observed only as the first approximation for compound lipophilicity, bioaccumulation and toxicity in fish, and sorption to soil and sediments, it assumes that lipophilicity is the main factor of anti-microbial activity [44,56]. Nevertheless, aiming at a deeper understanding of the specific mechanistic description of IL eco-toxicity, it is worth considering that the ionic liquid properties are more comprehensively quantified through lipophilicity, polarizability and total energy as a unitarily complex of factors in developing appropriate structure-activity relationship (SAR) studies. However, the main problem in assessing the viable QSAR studies for predicting ionic liquid toxicities concerns the *anionic-cationic interaction* superimposed on the anionic and cationic subsystems containing ionic liquids. There are two main complementary ways of attaining this goal [27,28,30]. One may address the search of special rules for assessing the anionic-cationic structural separately from the individual anionic and cationic ones and later generating the QSAR models – the so-called mod-

el $|1+\rangle$. Otherwise, when the so-called internal angle of ionic liquids sub-systems (cation and anion), eq. (30), is high enough that a sort of "resonance effects" would appear between them, that outcome should be avoided by considering structural parameter composition (superposition, as orthogonal states in quantum mechanics) such that it constitutes the way of parameter depending the predicted endpoints, that is, the so-called causal model $|0+\rangle$. Together, these properties may be unitarily expressed by the operatorial equation

$$\hat{O}_{S-SAR}\left|0+\right\rangle \begin{cases} = \left|1+\right\rangle, & \text{fixed endpoints} \\ = \left|0+\right\rangle, & \text{path endpoints} \end{cases} \tag{41}$$

with the Spectral-SAR operator, consistently defined by the successive rules:

$$\hat{O}_{S-SAR} : \begin{cases} Det\left(\left|Y\right\rangle, \left|X_0\right\rangle, \left|X_1\right\rangle, ..., \left|X_M\right\rangle\right) = 0, \left\|Y\right\rangle\|, r_{S-SAR}^{ALGEBRAIC}, \\ \delta\left[A_{(\|\bullet\|_r)}, B_{(\|\bullet\|_r)}\right] = 0, \left\langle\alpha, \beta, \gamma, ...\right\rangle, \quad A, B : ENDPOINTS \\ \qquad\qquad\qquad\qquad\qquad\qquad \alpha, \beta, \gamma, ... : SPECTRAL\ PATHS \end{cases} \tag{42}$$

that widely fulfill the principles of green chemistry specialized to the OECD-QSAR principles and here manifested as Spectral-SAR ecotoxicological principles. These equations are able to offer the complete picture of molecular specific interaction between a series of chemicals with certain species by generating the molecular mechanisms of actions; also, they are opening room for preventing and controlling the envisaged bio- and ecological systems.

Note that the presented Spectral-SAR methodology provides the possibility of analytical characterizing the bio-and eco- activity of other species against given a set of trained or new synthesized chemicals and for the inter-species correlations; it has, beyond giving quantitatively similar results as the already traditional regression QSAR methods [106], many practical advantages, namely [97]:

- it has the strength of no dependency on the way in which the input data are considered, thus being largely independent of the outliers detection [26,30];

- it uses the algebraically instead of statistically recipe to furnish a generalized view for the "intensity" of chemical-biological interaction, through the vectors, predicted norms $\|\left|Y\right\rangle\|$, and of their properties in generalized multi-dimensional orthogonal spaces [69];

- it is also easily applicable to the case where the number of structural parameters exceeds those of the available biological activities, a situation more often observed in actual practice but being still an open problem in QSAR, due to the statistically forbidden condition that such situations imply [98];

- it is also able to furnish the key in treating the so-called spectral analysis of the activity itself through *action norm* and its *least activity path principle* (i.e., $\delta\|\left|Y\right\rangle\| = 0$ over many

possible predicted end-points), thus providing the appropriate mechanistic picture of the envisaged ecotoxicity [26,30].
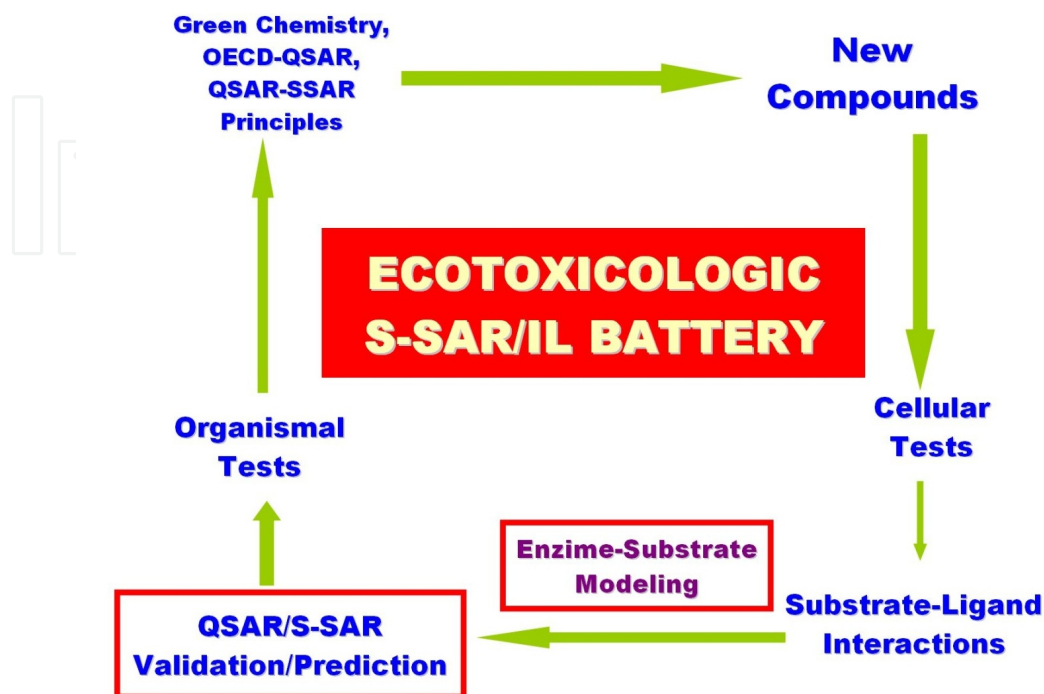

Figure 5. Conceptual description of an ecotoxicological battery constructed with the aid of QSAR/Spectral-SAR modeling of ionic liquids (IL) ligand interactions over cellular and later on organismal substrates to validate the toxicological safety of the newly synthesized compounds in accordance with the green chemistry, OECD-QSAR and, eventually, the QSAR/SSAR ecotoxicological principles.

In this way, the presented S-SAR model appears to provide a uniform picture of the anionic-cationic interaction in ionic liquids as conciliating the anionic and cationic effects observed to date. However, further studies on different species with diverse computational schemes and parameters are required, especially those that employ the quantum and algebraic features of the general operatorial equation derived in this study (41). Furthermore, by involving the enzyme-substrate modeling for receptor-effector interactions for biological activity driving chemical reactivity, as was recently reported [107], this study conceptually assessed a definitive theory of ionic liquid inter- and intra- mode of action such that it can be used for being integrated over a wide range of organisms toward designing specific eco-toxicological batteries [97], see Figure 5, for the ionic liquid's chemical-biological interactions.

Acknowledgements

Author details

Ana-Maria Putz[1,2] and Mihai V. Putz[2*]

*Address all correspondence to: mvputz@cbg.uvt.ro

1 Institute of Chemistry Timișoara of the Romanian Academy, Timișoara, Romania

2 Laboratory of Computational and Structural Physical Chemistry, Biology-Chemistry Department, West University of Timișoara, Romania

References

[1] Dahl, J. A., Maddux, B. L. S., & Hutchison, J. E. (2007). Toward Greener Nanosynthesis. *Chem Rev*, 107, 2228-2269.

[2] Liu, Z. M., & Sun, Z. Y. (2010). Green Solvent-Based Approaches for Synthesis of Nanomaterials. *Science China Chemistry*, 53, 372-382.

[3] Wilkes, J. S. (2002). A Short History of Ionic Liquids-From Molten Salts to Neoteric Solvents. *Green Chemistry*, 4, 73-80.

[4] Valkenburg, M. V., Vaughn, R. L., Williams, M., & Wilkes, J. S. (2005). Thermochemistry of Ionic Liquid Heat-Transfer Fluids. *Thermochimica Acta*, 425, 181-188.

[5] Zhou, Y. (2005). Recent Advances in Ionic Liquids for Synthesis of Inorganic Nanomaterials. *Current Nanoscience*, 1, 35-42.

[6] Sarbu, T., & Matyjaszewski, K. (2001). Macromolecular ATRP of Methyl Methacrylate in the Presence of Ionic Liquids with Ferrous and Cuprous Anions. *Chemical Physics*, 202, 3379-3391.

[7] Shamsipur, M., Beigi, A. A. M., Teymouri, M., Pourmortazavi, S. M., & Irandoust, M. (2010). Physical and Electrochemical Properties of Ionic Liquids 1-Ethyl-3-Methylimidazolium Tetrafluoroborate, 1-Butyl-3-Methylimidazolium Trifluoromethanesulfonate and 1-Butyl-1-Methylpyrrolidinium Bis (Trifluoromethylsulfonyl) Imide. *Journal of Molecular Liquids*, 157, 43-50.

[8] Karout, A., & Pierre, A. C. (2009). Silica Gelation Catalysis by Ionic Liquids. *Catalysis Communications*, 10, 359-361.

[9] Karout, A., & Pierre, A. C. (2009). Porous Texture of Silica Aerogels Made with Ionic Liquids as Gelation Catalysts. *Journal of Sol-Gel Science and Technology*, 49, 364-372.

[10] Wahab, M. A., Kim, I. I., & Ha, C. S. (2004). Hybrid Periodic Mesoporous Organosilica Materials Prepared from 1,2-bis(triethoxysilyl)ethane and (3- cyanopropyl)triethoxysilane. *Microporous and Mesoporous Materials*, 69, 19-27.

[11] Lebold, T. (2010). Mesoporous Silica Nanostructures: A Versatile Platform in Drug-Delivery and Material Science. *Dissertation zur Erlangung des Doktorgrades der Fakultät für Chemie und Pharmazie der Ludwig-Maximilians-Universität München*, http://edoc.ub.uni-muenchen.de/11819/1/Lebold_Timo.pdf, accessed 2 May 2011.

[12] Li, S., Liu, M., Zhang, A., & Guo, X. (2010). Spherical Mesoporous Silica Templated With Ionic Liquid and Cetyltrimethylammonium Bromide and Its Conversion to Hollow Spheres. *Materials Letters*, 64, 599-601.

[13] Wu, J., Liu, C., Jiang, Y., Hu, M., Li, S., & Zhai, Q. (2010). Synthesis of Chiral Epichlorohydrin By Chloroperoxidase-Catalyzed Epoxidation of 3-Chloropropene in the Presence of an Ionic Liquid as Co-Solvent. *Catalysis Communications*, 11, 727-731.

[14] Hu, J., Gao, F., Shang, Y., Peng, C., Liu, H., & Hu, Y. (2011). One-Step Synthesis of Micro/Mesoporous Material Templated by CTAB and Imidazole Ionic Liquid in Aqueous Solution. *Microporous and Mesoporous Materials*, 142, 268-275.

[15] Flannigan, D. J., Hopkins, S. D., & Suslick, K. S. (2005). Sonochemistry and Sonoluminescence in Ionic Liquids, Molten Salts, and Concentrated Electrolyte Solutions. *Journal of Organometallic Chemistry*, 690, 3513-3517.

[16] Bravo, J. L., Lopez, I., Cintas, P., Silvero, G., & Arevalo, M. J. (2006). Sonochemical Cycloadditions in Ionic Liquids. Lessons from Model Cases Involving Common Dienes and Carbonyl Dienophiles. *Ultrasonics Sonochemistry*, 13, 408-414.

[17] Mason, T. J. (1991). *Practical Sonochemistry. Users Guide to Applications in Chemistry and Chemical Engineering*, Chichester, Ellis Horwood, 22-23.

[18] Gobel, R., Hesemann, P., Weber, J., Moller, E., Friedrich, A., Beuermann, S., & Taubert, A. (2009). Surprisingly High, Bulk Liquid-Like Mobility of Silica-Confined Ionic Liquids. *Phys. Chem. Chem. Phys.*, 11, 3653-3662.

[19] Singh, M. P., Singh, R. K., & Chandra, S. (2010). Thermal Stability of Ionic Liquid in Confined Geometry. *Journal of Physics D: Applied Physics*, 43, 1-4.

[20] Wang, G., Otuonye, A. N., Blair, E. A., Denton, K., Tao, Z., & Asefa, T. (2009). Functionalized Mesoporous Materials for Adsorption and Release of Different Drug Molecules: A Comparative Study. *Journal of Solid State Chemistry*, 182, 1649-1660.

[21] Savii, C., & Putz, A. M. (2011). Advances In (Bio)Responsive Nanomaterials. *In: Putz M.V. (ed.) Carbon Bonding and Structures: Advances in Physics and Chemistry*, Berlin-London-New York, Springer Verlag, 379-435.

[22] Putz, A. M., Ianasi, C., Dascalu, D., Savii, C., & Sfirloaga, P. (2008, 6-7 November 2008). Comparative Studies of Sonogels and Xerogels Synthesized with 1-Butyl-4-Methylpyridinium Tetrafluoroborate Ionic Liquid. Timișoara, Romania. *Proceedings of New Trends and Strategies in the Chemistry of Advanced materials with Relevance in Biological Systems, Technique and Environmental Protection*, Timișoara, Mirton Publishing House, 90-100.

[23] Putz, A. M., Ianăşi, C., Dascălu, D., & Savii, C. (2010). Acid Catalysed Silica Xerogels and Sonogels Synthesized with Buty-4-Methypyridinium Telrafluoroborate Ionic Liquid. *International Journal of Environmental Sciences*, 1, 79-88.

[24] Ianasi, C., Putz, A. M., Dascalu, D., & Savii, C. (2009, 28 September 2009). ILs Assisted Silica Mesoporous Sonogels Synthesis And Porosity Characterization. Szeged, Hungary. *In: Zoltán Galbács (ed.) Proceedings of the 16ʰ Symposium on Analytical and Environmental Problems*.

[25] Ianasi, C., Putz, A. M., & Savii, C. (2009, 5-6 November). Approximation of Silica Xerogels And Sonogels Texture Parameters Dependence On Synthesis Variables: ILs:Si mole ratio. Timişoara, Romania. *Proceedings of the Symposium New trends and strategies in the chemistry of advanced materials with relevance in biological systems, technique and enviromental protection*, Timişoara, Mirton Publishing House, 161-164.

[26] Putz, M. V., & Lacrămă, A. M. (2007). Introducing Spectral Structure Activity Relationship (S-SAR) Analysis. Application to Ecotoxicology. *International Journal of Molecular Sciences*, 8, 363-391.

[27] Lacrămă, A.-M., Putz, M. V., & Ostafe, V. (2007). A Spectral-SAR Model for the Anionic-Cationic Interaction in Ionic Liquids: Application to Vibrio fischeri Ecotoxicity. *International Journal of Molecular Sciences*, 8, 842-863.

[28] Putz, M. V., Lacrămă, A.-M., & Ostafe, V. (2007). *Spectral-SAR Ecotoxicology of Ionic Liquids. The Daphnia magna Case, International Journal of Ecology (former Research Letters in Ecology)*, Article ID12813, 5 pages, DOI:10.1155/2007/12813.

[29] Chicu, S. A., & Putz, M. V. (2009). Köln-Timişoara Molecular Activity Combined Models toward Interspecies Toxicity Assessment. *International Journal of Molecular Sciences*, 10, 4474-4497.

[30] Putz, M. V. (2012). *QSAR & SPECTRAL-SAR in Computational Ecotoxicology*, Toronto & New Jersey, Apple Academics & CRC Press- Taylor & Francis Group.

[31] Putz, M. V., Lacrămă, A. M., & Ostafe, V. (2006). Full Analytic Progress Curves of Enzymic Reaction in Vitro. *International Journal of Molecular Sciences*, 7, 469-484.

[32] Putz, M. V., & Lacrămă, A.-M. (2007). Enzymatic Control of The Bio-Inspired Nanomaterials at The Spectroscopic Level. *Journal of Optoelectronics and Advanced Materials*, 9, 2529-2534.

[33] Putz, M. V., Lacrămă, A.M., & Ostafe, V. (2007). Introducing Logistic Enzyme Kinetics. *Journal of Optoelectronics and Advanced Materials*, 9, 2910-2916.

[34] Putz, M. V. (2011). On Reducible Character of Haldane-Radić Enzyme Kinetics to Conventional and Logistic Michaelis-Menten Models. *Molecules*, 16, 3128-3145.

[35] Putz, M. V., & Putz, A. M. (2011). Logistic vs. W-Lambert Information in Quantum Modeling of Enzyme Kinetics. *International Journal of Chemoinformatics and Chemical Engineering*, 1, 42-60.

[36] Lacrămă, A. M., Putz, M. V., & Ostafe, V. (2005). New Enzymatic Kinetic Relating Michaelis-Menten Mechanisms. *Annals of West University of Timişoara-Series of Chemistry*, 14, 179-190.

[37] Lacrămă, A. M., Putz, M. V., & Ostafe, V. (2006). Studies of Lactate Dehidrogenase from Different Species and Use of The Enzyme In Ecotoxicologically Test Batteries. *Monographs Series of Annals of West University of Timisoara, Series of Biochemistry* [5], 1584-1227.

[38] Lacrămă, A. M., Popet, L., & Ostafe, V. (2007). Use of Catalase from Spinach for Testing at Molecular Level the Toxicity of Some Ionic Liquids. *Annals of West University of Timişoara- Series of Chemistry*, 16, 191-200.

[39] Lacrămă, A. M. (2007). Ecotoxicological Batteries with Organisms from Different Species. *PhD Thesis*, West University of Timisoara.

[40] Putz, M. V., Putz, A.-M., Ostafe, V., & Chiriac, A. (2010). Spectral-SAR Ecotoxicology of Ionic Liquids-Acetylcholine Interaction on E. Electricus Species. *International Journal of Chemical Modeling*, 2, 85-96.

[41] Mincea, M., Lacrămă, A. M., & Ostafe, V. (2004). Use of Bovine Liver Alkaline Phosphatase for Testing at Molecular Level the Toxicity of Chemical Compunds. *Annals of West University of Timişoara-Series Chemistry*, 13, 87-98.

[42] Mincea, M., Lacrămă, A. M., Stoian, C., Baicu, I., Nemes, N., Popet, L., & Ostafe, V. (2005, 24-25 February). Multienzimatic Test Battery-a Model for Testing at Molecular Level the Toxicity of Chemical Compounds. Timişoara, Romania. *In: Ionel I. (ed.) Humboldt Sustainability for Humanity and Environment in the Extended Connection Field Science-Economy-Policy*, Timişoara, Polytechnic Publishing House, II, 211-214.

[43] Pernak, J., & Chwala, P. (2003). Synthesis and Anti-Microbial Activities of Choline-Like Quaternary Ammonium Chlorides. *European Journal of Medicinal Chemistry*, 38, 1035-1042.

[44] Pernak, J., Sobaszkiewicz, K., & Mirska, I. (2003). Antimicrobial Activities of Ionic Liquids. *Green Chemistry*, 5, 52-56.

[45] Docherty, K. M., & Kulpa, C. F., Jr. (2005). Toxicity and Antimicrobial Activity of Imidazolium and Pyridinium Ionic Liquids. *Green Chemistry*, 7, 185-189.

[46] Docherty, K. M., Hebbeler, S. Z., & Kulpa, C. F., Jr. (2006). An Assessment of Ionic Liquid Mutagenicity Using the Ames Test. *Green Chemistry*, 8, 560-567.

[47] Bernot, R. J., Brueseke, M. A., Evans-White, M. A., & Lamberti, G. A. (2005). Acute and Chronic Toxicity of Imidazolium-Based Ionic Liquids on Daphnia Magna. *Environmental Toxicology and Chemistry*, 24, 87-92.

[48] Bernot, R. J., Kennedy, E. E., & Lamberti, G. A. (2005). Effects of Ionic Liquids on the Survival, Movement, and Feeding Behavior of the Freshwater Snail, Physa Acuta. *Environmental Toxicology and Chemistry*, 24, 1759-1765.

[49] Couling, D. J., Bernot, A. R., Docherty, K. M., Dixon, J. K., & Maginn, E. J. (2006). Assessing the Factors Responsible for Ionic Liquid Toxicity to Aquatic Organisms Via Quantitative Structure- Property Relationship Modeling. *Green Chemistry*, 8, 82-90.

[50] Garcia, M. T., Gathergood, N., & Scammells, P. J. (2005). Biodegradable Ionic Liquids. Part II. Effect of the Anion and Toxicology. *Green Chemistry*, 7, 9-14.

[51] Stock, F., Hoffmann, J., Ranke, J., Stormann, R., Ondruschka, B., & Jastorff, B. (2004). Effects of Ionic Liquids on the Acetylcholinesterase- A Structure-Activity Relationship Consideration. *Green Chemistry*, 6, 286-290.

[52] Shugart, L. (1996). Molecular Markers to Toxic Agents. *In: Newman Mc, Jagoe Ch. (eds.), Ecotoxicology: A Hierarchical Treatment*, Boca Raton, Lewis, 133-161.

[53] Newman, M., & Dixon, P. (1996). Ecologically Meaningful Estimates of Lethal Effect in Individuals. *In: Newman Mc, Jagoe Ch. (eds.), Ecotoxicology: A Hierarchical Treatment*, Boca Raton, Lewis, 225-253.

[54] Jastorff, B., Molter, K., Behrend, P., Bottin-Weber, U., Filser, J., Heimers, A., Ondurschka, B., Ranke, J., Scaefer, M., Schroder, H., Stark, A., Stepnowski, P., Stock, F., Stormann, R., Stolte, S., Welz-Biermann, U., Ziegert, S., & Thoming, J. (2005). Progress in Evaluation of Risk Potential of Ionic Liquids-Basis for an Eco-design of Sustainable Products. *Green Chemistry*, 7, 362-372.

[55] Stepnowski, P., Skladanowski, A. C., Ludwiczak, A., & Laczynska, E. (2004). Evaluating the Cytotoxicity of Ionic Liquids Using Human Cell Line Hela. *Human and Experimental Toxicology*, 23, 513-517.

[56] Jastorff, B., Stormann, R., Ranke, J., Molter, K., Stock, F., Oberheitmann, B., Hoffmann, W., Hoffmann, J., Nuchter, M., Ondruschka, B., & Filser, J. (2003). How Hazardous are Ionic Liquids? Structure- Activity Relationship and Biologic Testing as Important Elements for Sustainability Evaluation. *Green Chemistry*, 5, 136-142.

[57] Hansh, C., & Leo, A. (1995). Exploring QSAR Washington ACS Professional Reference Book.

[58] Swatloski, R. P., Holbrey, J. D., & Rogers, R. D. (2003). Ionic Liquids Are Not Always Green: Hydrolysis of 1-Butyl-3-Methylimidazolium Hexafluorophosphate. *Green Chemistry*, 5, 361-363.

[59] Swatloski, R. P., Holbrey, J. D., Memon, S. B., Caldwell, G. A., Caldwell, K. A., & Rogers, R. D. (2004). Using Caenorhabditis Elegans to Probe Toxicity Of 1-Alkyl-3-Methylimidazolium Chloride Based Ionic Liquids. . ChemInform DOI:10.1002/chin. 200428226 , 35

[60] Hunt, P. A. (2006). The Simulation of Imidazolium-Based Ionic Liquids. *Molecular Simulation*, 32, 1-10.

[61] Hunt, P. A., & Gould, I. R. (2006). Structural Characterization of the 1-Butyl-3-Methylimidazolium Chloride Ion Pair Using Ab Initio Methods. *Journal of Physical Chemistry A*, 110, 2269-2282.

[62] Hunt, P. A., Gould, I. R., & Kirchner, B. (2007). The Structure of Imidazolium-Based Ionic Liquids: Insights from Ion-Pair Interactions. *Aust. J. Chem.*, 60, 9-14.

[63] Hunt, P. A., Kirchner, B., & Welton, T. (2006). Characterising the Electronic Structure of Ionic Liquids: An Examination of the 1-Butyl-3-ethylimidazolium Chloride Ion Pair. *Chemical European Journal*, 12, 6762-6775.

[64] Ropel, R., Belveze, L. S., Aki, S. N. V. K., Stadtherr, M. A., & Brennecke, J. F. (2005). Octanol-Water Partition Coefficients of Imidazolium-Based Ionic Liquids. *Green Chemistry*, 7, 83-90.

[65] Wells, A. S., & Coombe, V. T. (2006). On the Freshwater Ecotoxicity and Biodegradation Properties of Some Common Ionic Liquids. *Organic Process Research and Development*, 10, 794-798.

[66] Anastas, P. T., & Warner, J. C. (1998). *Green Chemistry Theory and Practice*, New York, Oxford University Press.

[67] National Toxicology Program (NTP) and National Institute of Environmental Health Sciences (NIEHS). (2004). *Review of Toxicological Literature for Ionic Liquids*, Prepared By Integrated Laboratory Systems Inc., Research Triangle Park, NC.

[68] Kamrin, M. A. (1997). *Pesticide Profiles: Toxicity, Environmental Impact, and Fate*, Boca Raton, Lewis Publishers.

[69] Putz, M. V., & Putz, A. M. (2011). Timişoara Spectral- Structure Activity Relationship (Spectral-SAR) Algorithm: From Statistical and Algebraic Fundamentals to Quantum Consequences. *In: Mihai V. Putz (ed.), Quantum Frontiers of Atoms and Molecules*, New York, NOVA Science Publishers, Inc., 539-580.

[70] Putz, M. V. (2012). Chemical Orthogonal Spaces. *In: Mathematical Chemistry Monographs of MATCH-Commun. Math. Comput. Chem.*, Kragujevac University Press, Kragujevac, in preparation, to be submitted, 14, http://www.pmf.kg.ac.rs/match/mcm14.html.

[71] Dirac, P. A. M. (1944). *The Principles of Quantum Mechanics*, Oxford, Oxford University Press.

[72] Randić, M. (1991). Resolution of Ambiguities in Structure-Property Studies by Use of Orthogonal Descriptors. *J. Chem. Inf. Comput. Sci.*, 31, 311-320.

[73] Randić, M. (1991). Orthogonal Molecular Descriptors. *New Journal of Chemistry*, 15, 517-525.

[74] Fadeeva, V. N. (1959). *Computational Methods of Linear Algebra*, New York, Dover Publications.

[75] Steen, L. A. (1973). Highlights in the History of Spectral Theory. *The American Mathematical Monthly*, 80, 359-381.

[76] Siegmund-Schultze, R. (1986). Der Beweis des Hilbert-Schmidt Theorem. *Archive for History of Exact Sciences*, 36, 251-270.

[77] Anderson, T. W. (1958). *An Introduction to Multivariate Statistical Methods*, New York, Wiley.

[78] Draper, N. R., & Smith, H. (1966). *Applied Regression Analysis*, New York, Wiley.

[79] Box, G. E. P., Hunter, W. G., & Hunter, J. S. (1978). *Statistics for Experimenters*, New York, John-Wiley.

[80] Green, J. R., & Margerison, D. (1978). *Statistical Treatment of Experimental Data*, New York, Elsevier.

[81] Topliss, J. (1983). *Quantitative Structure-Activity Relationships of Drugs*, New York, Academic Press.

[82] Seyfel, J. K. (1985). QSAR and Strategies in the Design of Bioactive Compounds. New York, VCH Weinheim.

[83] Chatterjee, S., Hadi, A. S., & Price, B. (2000). *Regression Analysis by Examples* (3rd Ed.), New York, John-Wiley.

[84] Amić, D., Davidović-Amić, D., & Trinajstić, N. (1995). Calculation of Retention Times of Anthocyanins with Orthogonalized Topological Indices. *Journal of Chemical Information and Computer Science*, 35, 136-139.

[85] Lučić, B., Nikolić, S., Trinajstić, N., & Juretić, D. (1995). The Structure-Property Models Can Be Improved Using The Orthogonalized Descriptors. *Journal of Chemical Information and Computer Science*, 35, 532-538.

[86] Šoškić, M., Plavšić, D., & Trinajstić, N. (1996). Link Between Orthogonal and Standard Multiple Linear Regression Models. *Journal of Chemical Information and Computer Science*, 36, 829-832.

[87] Klein, D. J., Randić, M., Babić, D., Lučić, B., Nikolić, S., & Trinajstić, N. (1997). Hierarchical Orthogonalization of Descriptors. *International Journal of Quantum Chemistry*, 63, 215-222.

[88] Putz, M. V. (2010). Cosmos, Order and Obligations: The Big CO2. *International Journal of Environmental Sciences*, 1, 1-8.

[89] Ritter, S. K. (2008). Calling all Chemists. *Chemical and Engineering News*, 18, 59-68.

[90] Anastas, P. T., Levy, I. J., & Parent, K. E. (2009). Green Chemistry Education: Changing the Course of Chemistry. *ACS Symposium Series. 1011*, Washington, DC, American Chemical Society, DOI:10.1021/bk-2009-1011.

[91] Anastas, P. T., & Zimmerman, J. B. (2003). Design through the Twelve Principles of Green Engineering. *Environmental Science and Technology*, 37, 94A-101A.

[92] OECD. (2004). *Report from the Expert Group on (Quantitative) Structure-Activity Relationships [(Q)SARs] on the Principles for the Validation of (Q)SARs, Series on Testing and Assessment* [49], 206, Paris, http://www.oecd.org/document/30/0,2340,en_2649_34365_1916638_1_1_1_1.html, accessed 3 March 2011.

[93] OECD. (2005). *Guidance Document on the Validation and International Acceptance of New or Updated Test Methods for Hazard Assessment, Series on Testing and Assessment* [34], 96, Paris, http://www.oecd.org/document/30/0,2340,en_2649_34365_1916638_1_1_1_1,00.html, accessed 3 March 2011.

[94] OECD. (2006). *Report on the Regulatory Uses and Applications in OECD Member Countries of (Quantitative) Structure-Activity Relationship [(Q)SAR] Models in the Assessment of New and Existing Chemicals, Series on Testing and Assessment* [58], 79, Paris, http://www.oecd.org/document/30/0,2340,en_2649_34365_1916638_1_1_1_1,00.html, accessed 3 March 2011.

[95] OECD. (2007). *Guidance Document on the Validation of (Quantitative) Structure-Activity Relationship [(Q)SAR] Models, Series on Testing and Assessment* [69], 154, Paris, http://www.oecd.org/document/30/0,2340,en_2649_34365_html, accessed 3 March 2011.

[96] Putz, M. V., Putz, A. M., & Barou, R. (2011). Spectral-SAR Realization of OECD-QSAR Principles. *International Journal of Chemical Modeling*, 3, 173-190.

[97] Lacrămă, A. M., Putz, M. V., & Ostafe, V. (2007). Designing a Spectral Structure-Activity Ecotoxico-Logistical Battery. *In: Putz M.V. (Ed.), Advances in Quantum Chemical Bonding Structures. Kerala: Research Signpost*, 389-419.

[98] Putz, M. V., Putz, A. M., Lazea, M., & Chiriac, A. (2009). Spectral vs. Statistic Approach of Structure-Activity Relationship. Application on Ecotoxicity of Aliphatic Amines. *Journal of Theoretical and Computational Chemistry*, 8, 1235-1251.

[99] Putz, M. V., Duda-Seiman, C., Duda-Seiman, D. M., & Putz, A.-M. (2008). Turning SPECTRAL-SAR into 3D-QSAR Analysis. Application on H+K+-ATPase Inhibitory Activity. *International Journal of Chemical Modeling*, 1, 45-62.

[100] Kaiser, K. L. E., & Palabrica, V. S. (1991). Photobacterium phosphoreum Toxicity Data Index. *Water Pollution Research Journal of Canada*, 26, 361-431.

[101] Ranke, J., Mölter, K., Stock, F., Bottin-Weber, U., Poczobutt, J., Hoffmann, J., Ondruschka, B., Filser, J., & Jastorff, B. (2004). Biological Effects of Imidazolium Ionic Liquids with Varying Chain Lengths in Acute Vibrio Fischeri and Wst-1 Cell Viability Assays. *Ecotoxicology and Environmental Safety*, 58, 396-404.

[102] Mc Queen, D. J., Post, J. R., Mills, E. L., & Fish, C. J. (1986). Trophic Relationships in Freshwater Pelagic Eco-systems. *Can. J. Fish. Aquat. Sci.*, 43, 1571-1581.

[103] Hypercube, Inc. (2002). *HyperChem 7.01. Program package, Semiempirical, AM1, Polak-Ribier optimization procedure*.

[104] Sheldon, R. A. (2005). Green Solvents for Sustainable Organic Synthesis: State of The Art. *Green Chemistry*, 7, 267-278.

[105] Freemantle, M. (2007). New Frontiers for Ionic Liquids. *Chemical Engineering and News*, 1, 23-26.

[106] Miller, J. N., & Miller, J. C. (2000). *Statistics and Chemometrics for Analytical Chemistry*, Harlow, Pretience Hall, fourth edition.

[107] Putz, M. V., & Putz, A. M. (2013). DFT Chemical Reactivity Driven by Biological Activity: Applications for the Toxicological Fate of Chlorinated PAHs. *In: Putz M.V. & Mingos D.M.P. (eds.) Applications of Density Functional Theory to Biological and Bioinorganic Chemistry. Structure & Bonding*, 150.